The University of Manitoba

A CONFORMATIONAL STUDY OF 1-(β-D-ARABINOFURANOSYL) URACIL AND 2,2'-ANHYDRO-1-(β-D-ARABINOFURANOSYL) URACIL BY PROTON MAGNETIC RESONANCE SPECTROSCOPY

by

James Gordon Dalton

A Thesis

Submitted to

the Faculty of Graduate Studies and Research

University of Manitoba

in Partial Fulfillment

of the Requirements for the Degree

MASTER OF SCIENCE

Winnipeg, Manitoba

August, 1971

ACKNOWLDEGEMENTS

A special thanks to Dr.F.Hruska for his guidance throughout this study.

Thanks also to Mr.A.Mak whose assistance with the computer simulations saved many valuable hours, and Mr.B.Eagleson for his help with the figures.

I am indebted to the University of Manitoba for a Manitoba Fellowship Winter Stipend (1970-71), and to Dr.Hruska for financial support during the summer months.

ABSTRACT

A proton magnetic resonance study of 1-(β-D-arabinofuranosyl) uracil (aU) and 2,2'-anhydro-1-(β-D-arabinofuranosyl) uracil (cU) has been completed. On the basis of the coupling constants and chemical shifts measured for these two molecules a conformation is assigned to each. The β-anomer of aU is shown to exist in the anti conformation with greater restriction of rotation about the N-glycosyl bond than in U. Coupling constants between furanose protons indicate that the O-endo (^{O}V) conformation is favoured, and that the gauche-gauche rotamer is preferred by the exocyclic CH_2OH group. The β-anomer of cU is locked with the base at right angles to the anti position, due to the C_2-O-C_2, linkage. The furanose ring appears to favour the C_1,-exo (V_1) conformation, while the exocylic group still favours the gauche-gauche rotamer, although less so than in aU. A temperature-dependence observed for several shifts and coupling constants, and several previously-unreported long-range couplings, are related to structural features of these molecules.

TABLE OF CONTENTS

CHAPTER		PAGE
I	INTRODUCTION.....	1
II	NATURE OF THE PROBLEM.....	6
III	A BRIEF REVIEW OF NMR AS APPLIED TO CONFORMATIONAL STUDIES	
	A. Introduction.....	14
	B. Factors Affecting The Chemical Shift.....	16
	C. Correlation Of Coupling Constants With Structure	
	1. Geminal.....	22
	2. Vicinal.....	23
	3. Long-range.....	27
IV	EXPERIMENTAL.....	31
V	RESULTS AND DISCUSSION	
	A. Arabinouridine	
	1. Spectral Assignment.....	36
	2. Anomeric Configuration.....	43
	3. The Sugar-Base Torsion Angle.....	44
	4. Conformation Of The Furanose Ring.....	48
	5. Conformation Of The Exocyclic CH_2OH Group.....	55
	6. Evidence For The Presence Of Several Long-Range Couplings.....	59

CHAPTER PAGE

B. Anhydrouridine

1. Spectral Assignment..... 63

2. Anomeric Configuration And Sugar-Base Torsion Angle..... 75

3. Conformation Of The Furanose Ring..... 76

4. Conformation Of The Exocyclic CH_2OH Group..... 80

5. Evidence For A Number Of Long-Range Couplings..... 82

VI SUMMARY AND CONCLUSIONS..... 87

VII SUGGESTIONS FOR FUTURE RESEARCH..... 90

LIST OF TABLES

TABLE		PAGE
I	Calculated INDO Results for $^4J_{HH'}$ in Propane..	29
II	Chemical Shifts and Coupling Constants of aU..	40
IIIa	Calculated Dihedral Angles for the aU Furanose Ring.....	52
IIIb	Dihedral Angles for the Conformations of CYCLOPS.....	53
IV	Rotamer Populations for aU.....	58
V	Chemical Shifts and Coupling Constants of aU and cU.....	67
VI	Relative Shifts of the Sugar Protons in U, aU, and cU at 30°C.....	73
VIIa	Calculated Dihedral Angles for the cU Furanose Ring.....	77
VIIb	Dihedral Angles for the Conformations of CYCLOPS.....	78
VIII	Rotamer Populations for cU.....	81

LIST OF FIGURES

FIGURE		PAGE
1.	Structures of the eight commonly-occuring nucleosides.....	3
2.	Structural formulae of uridine, arabino-uridine, and anhydrouridine.....	5
3.	Tautomeric forms of uridine.....	8
4.	The α-anomer and β-anomer of aU.....	9
5.	Furanose conformations in the CYCLOPS scheme..	10
6.	Conformational rotamers about the C_4,-C_5,bond.	11
7.	The sugar-base torsion angle.....	12
8.	Nodal cones of shielding for C=O and C=C.....	18
9.	Electric field shielding of C=O.....	20
10.	Plot of the Karplus relation for selected values of J^{o} and J^{180}.....	25
11.	Specification of the dihedral angles ϕ and ϕ'.	28
12.	The 100 MHz spectrum of aU at 5°C.....	37
13.	The 100 MHz spectrum of aU at 30°C.....	38
14.	The 100 MHz spectrum of aU at 80°C.....	39
15.	The α-anomer and β-anomer of aU.....	45
16.	Syn and anti configurations of aU.....	46
17.	Furanose conformations in the CYCLOPS scheme..	50
18.	Conformational Rotamers about the C_4,-C_5,bond.	57
19.	Two molecules which show evidence of a "through-space" coupling.....	61
20.	The 100 MHz spectrum of cU at 5°C.....	64

FIGURE PAGE

21. The 100 MHz spectrum of cU at 30°C..... 65

22. The 100 MHz spectrum of cU at 80°C..... 66

23. aU and cU viewed along the N_1 to $C_{1'}$ direction showing the relative positions of the base ring..... 71

24. Possible charge delocalization in cU..... 74

25. The effect of imperfect resolution on the apparent magnitude of splitting of resonances. 84

CHAPTER I

Introduction

A nuceloside is an N-glycoside of a heterocyclic base. The component sugars of primary biological interest are the D-ribose and D-2'-deoxyribose, while the most common bases are adenine, guanine, cytosine, uracil, and thymine. The sugar and base are attached by an N-glycosyl bond from the $C_{1'}$ of the pentose to the N_1 position of a pyrimidine or N_9 position of a purine base. The ribonucleosides adenosine, guanosine, cytidine, and uridine contain a D-ribose sugar, while the 2'-deoxyribonucleosides 2'-deoxyadenosine, 2'-deoxyquanosine, 2'-deoxycytidine, and thymidine contain a 2-deoxy-D-ribose sugar. Structures of these eight common nucleosides are shown in Figure 1.

Nucleosides are one of the most versatile and most essential biomolecules. Nucleotides - the sugar-O-phosphate esters of nucleosides - form the monomeric units from which DNA and RNA are constructed. These biopolymers are involved in the storage and transmission of genetic information. As parts of coenzymes, they participate in a large number of essential energy-transforming reactions and intermediary metabolic pathways.

In addition to these common nucleosides there are a number of rare nucleosides having altered bases, sugars, or sugar-base bonds. Some are naturally-occuring, such as the t-RNA component pseudouridine[1-7], the antibiotics puromycin and tubercidin[8], and the sponge

Figure 1

Structures of the eight common nucleosides.

RIBONUCLEOSIDES

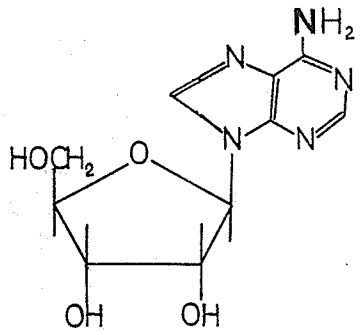

ADENOSINE

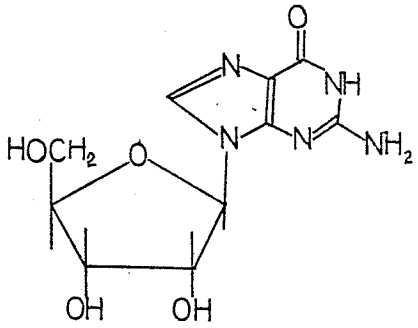

GUANOSINE

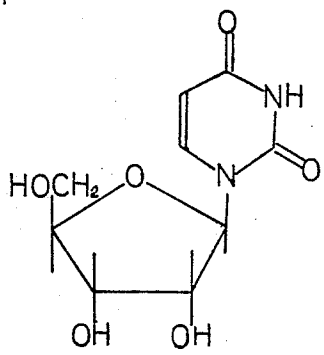

URIDINE

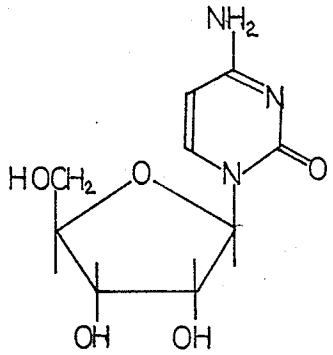

CYTIDINE

2'-DEOXYRIBONUCLEOSIDES

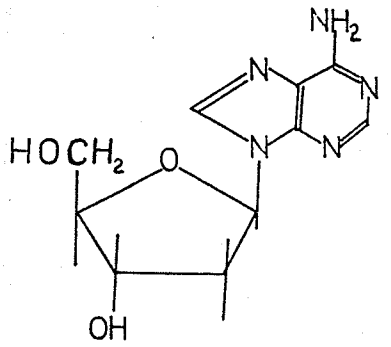

2'-DEOXYADENOSINE

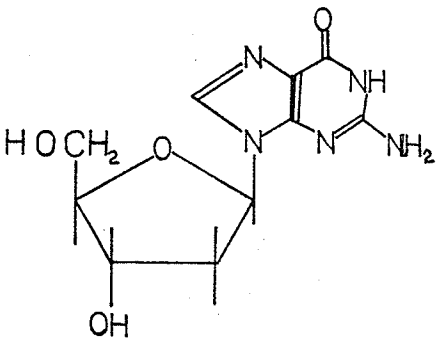

2'-DEOXYGUANOSINE

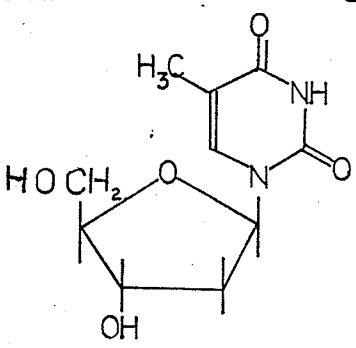

THYMIDINE

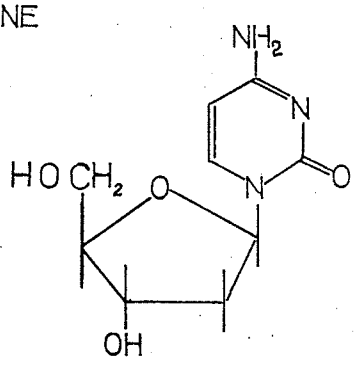

2' DEOXYCYTIDINE

derivatives aT *(spongothymidine) and aU *(spongouridine) [13-18,23-25]. Others are synthetic, but are important biologically as anti-metabolites or radiation sensitizers in treating malignant tumors[19-22], and important chemically as intermediates in the laboratory synthesis of other nucleosides, nucleotides and polynucleotides.

Arabinonucleosides have received considerable attention as antiviral[14] and anticancer drugs. Both aA and aC are inhibitors for DNA polymerase[9], and aA can replace the 3'-terminal adenosine in a still-chargeable t-RNA[11].

Polyarabinouridylic acid does not function as a messenger under conditions where polyuridylic acid does, and does not form a complex with polyadenylic acid[10]. These effects are ascribed to changes in secondary and tertiary structure due to the change in the position of the 2'-OH group from that occupied in the riboisomer (see Figure 2).

Interest in anhydronucleosides has arisen from their role as convenient precursors in the synthesis of the arabinonucleosides, - nucleotides, and polyarabinonucleotides.

* abbreviations used:
aU, aT, aA, aC for arabinouridine, - thymidine, - adenenosine, - cytidine
i.e. 1-(β-D-arabinofuranosyl) uracil, - thymine, - adenine, - cytosine
cU for anhydrouridine (2,2' - anhydro - 1-(β-D- arabinofuranosyl) uracil).

Figure 2

Structural formulae of uridine, arabinouridine, and anhydrouridine. The abbreviations in the square brackets, [ ], are those used throughout this paper.

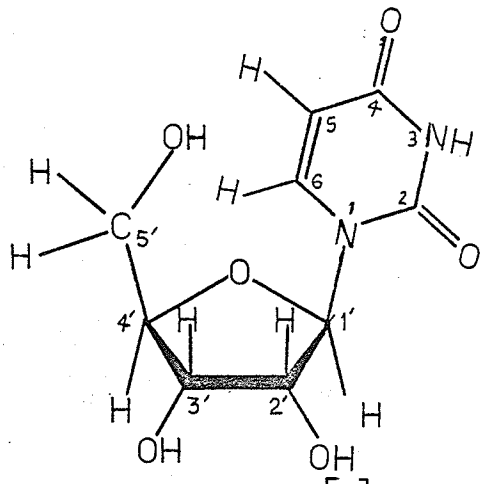

URIDINE [U]

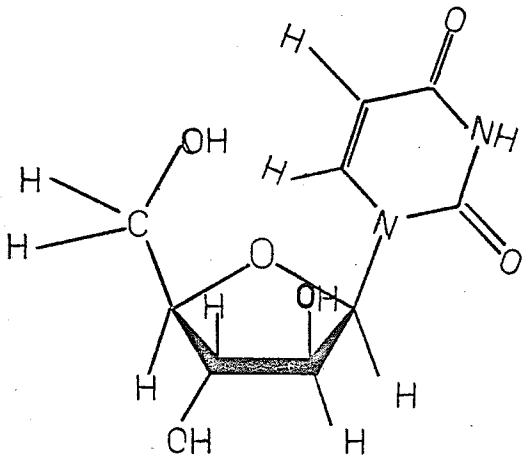

ARABINOURIDINE [aU]

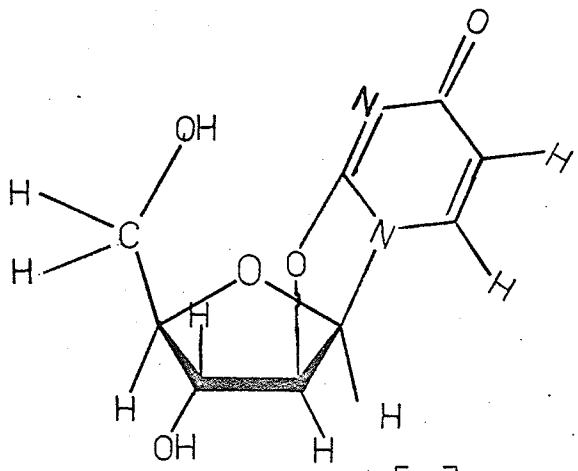

ANHYDROURIDINE [cU]

CHAPTER II

Nature of the Problem

The unusual properties of the arabinonucleosides and their polymers are usually attributed to structural changes due to the altered position of the 2'-OH. An ORD study by Maurizot et al.[12] of the conformational characteristics of arabinose- and ribose- containing dinucleoside phosphates led these authors to suggest an intramolecular hydrogen bond from the 2'-OH to an adjacent phosphate oxygen. However they note that an interaction involving the base, as in the hypothesis of Ts'O et al.[13] could not be excluded. Investigations by means of nuclear magnetic resonance (NMR)[15], optical rotatory dispersion (ORD) and circular dichroism (CD)[14] have yielded information concerning the sugar base torsion angle. To date, no complete structural analysis of arabinouridine has been published. This NMR study was undertaken with such an aim.

The heterocyclic base has been studied in some detail[29-42], indicating that at neutral pH the base exists as the diketo tautomer (Figure 3).

The structural parameters of interest are the anomeric configuration, the conformation of the furanose ring, the conformation of the exocyclic CH_2OH group, and the sugar-base torsion angle. These terms are defined in Figures 4-7 and the accompanying captions.

Figure 3

Tautomeric forms of uridine, with the diketo form, shown on the right, being the predominant form at neutral pH.

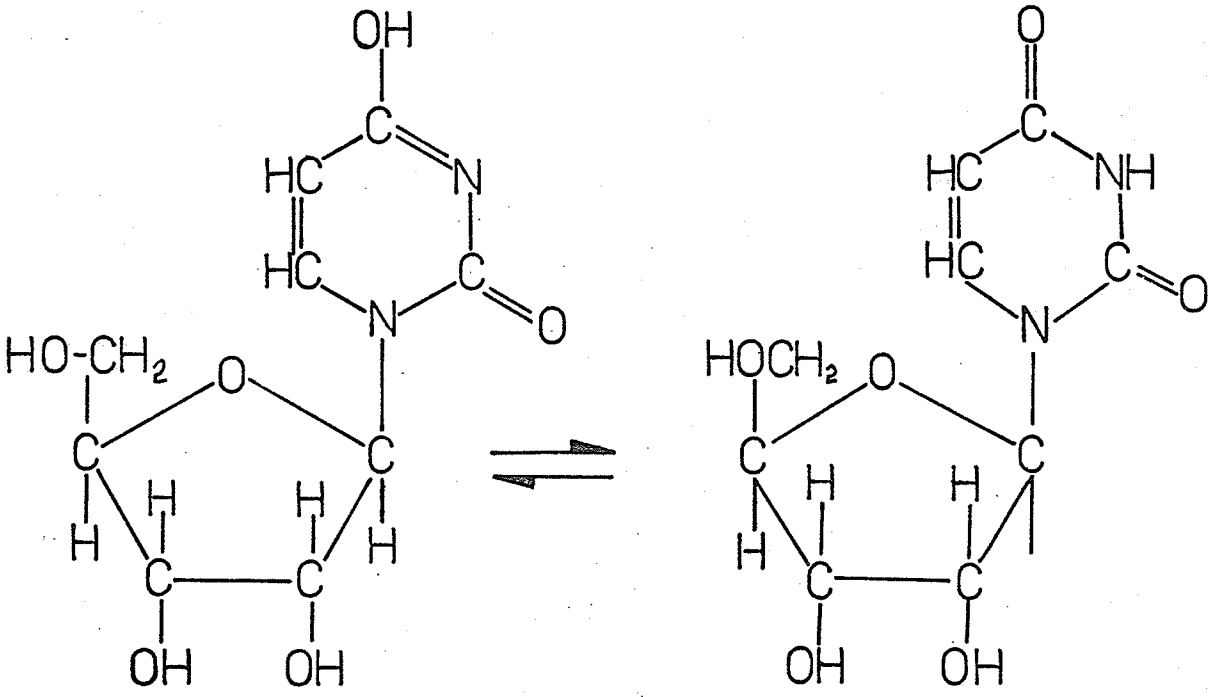
OH
C
HC
N
HC
C
O
N
HO-CH2
O
C
C
H
H
H
H
C
C
OH
OH
O
C
HC
NH
HC
C
O
N
HOCH2
O
C
C
H
H
H
H
C
C
OH
OH

Figure 4

The α-anomer and β-anomer of aU.

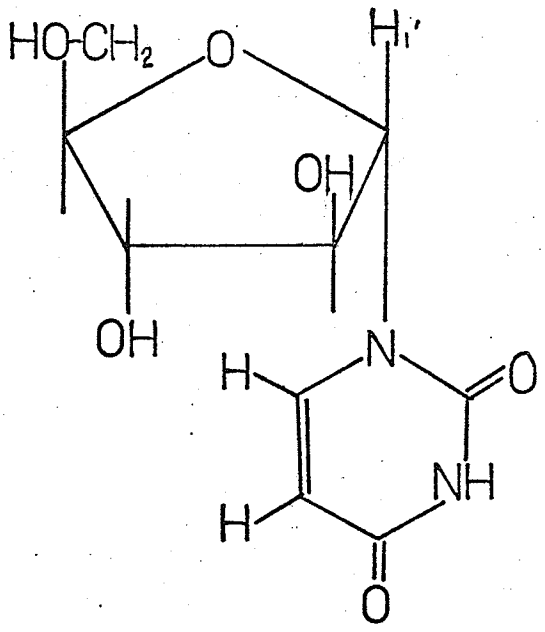

∝- aU

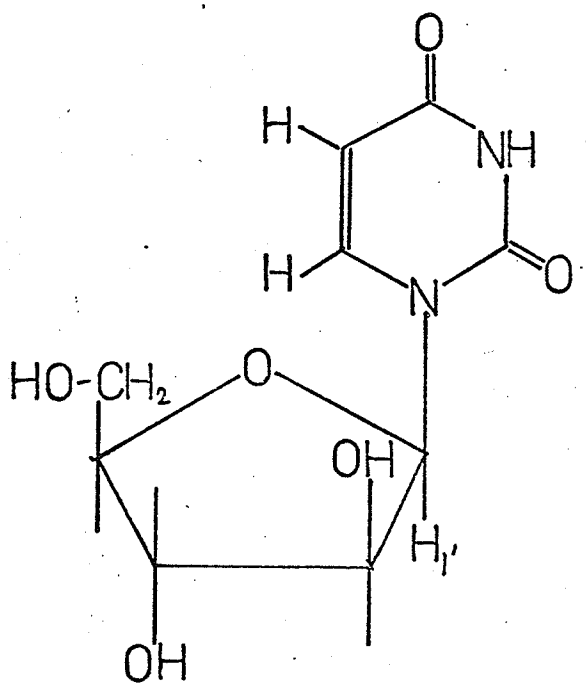

β - aU

Figure 5

Possible puckered furanose conformations indicated by the convention of Hall et al.[67]. ^{x}V or V_{y} indicates the "envelope" conformation in which the atom indicated by the superscript (or subscript) is above (or below) the plane defined by the remaining four atoms. $^{x}T_{y}$ indicates the "twist" conformation in which the two atoms designated by the superscript and subscript are respectively above and below the plane of the other three atoms. The CYCLe Of PSeudorotation (CYCLOPS) shows the possible equilibria by which all possible conformations can be achieved without ever passing through a completely planar molecule. The two molecules in the lower part of the diagram illustrate portions of the cycle.

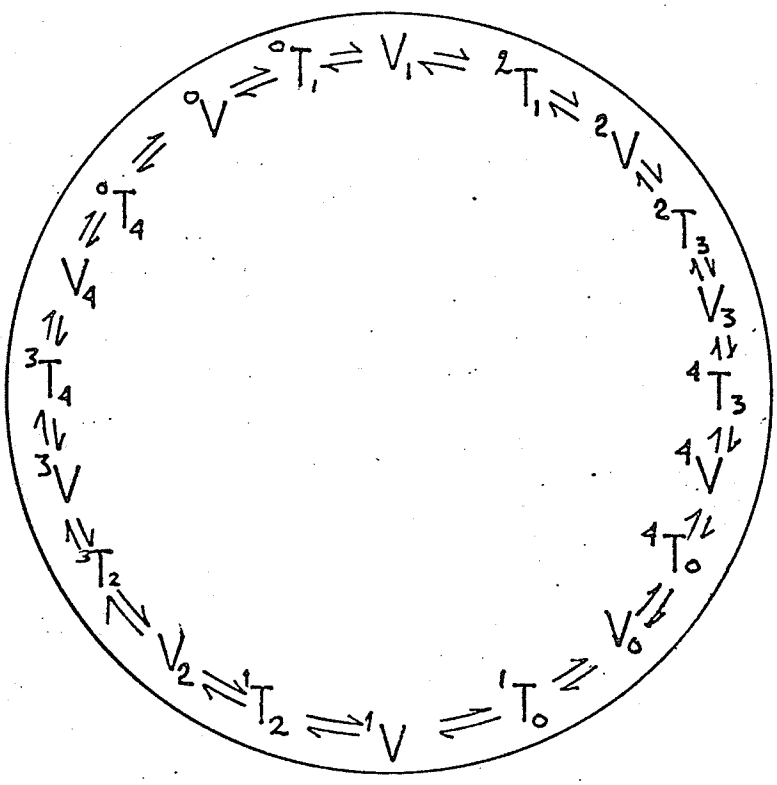

CYCLOPS

$^{\circ}V \equiv$

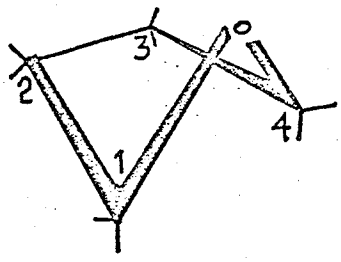

$^{1}V \equiv$

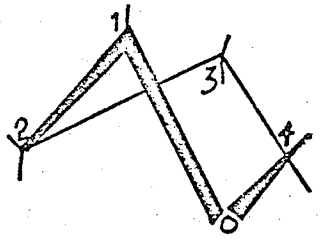

Figure 6

Newman projections showing the three possible rotamers about the exocyclic C_4'-C_5' bond, looking from C_5' toward C_4'.

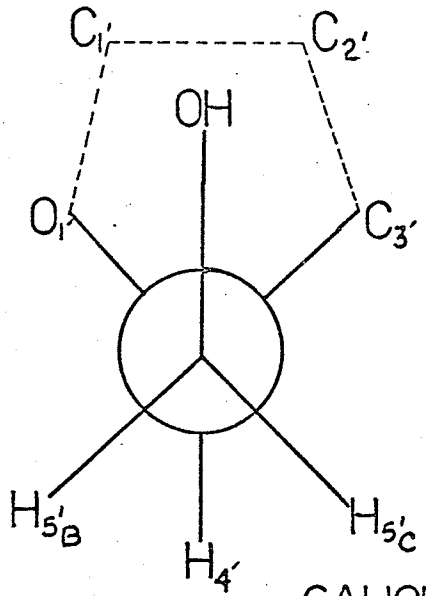

GAUCHE - GAUCHE

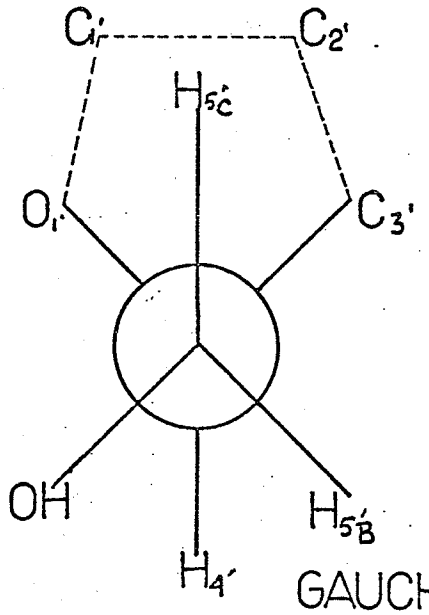

GAUCHE - TRANS

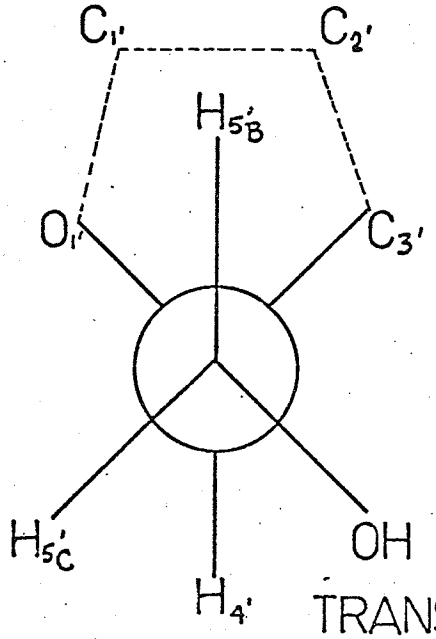

TRANS - GAUCHE

Figure 7

The sugar-base torsion angle, defined[77] as zero when the C_2 oxygen and the furanose oxygen are exactly opposite when viewed from above, positive values measured in a clockwise direction. Syn and anti refer to the values of ϕ_{CN} from -90° to $+90^{\circ}$ through 180°, and -90° to $+90^{\circ}$ through 0° respectively.

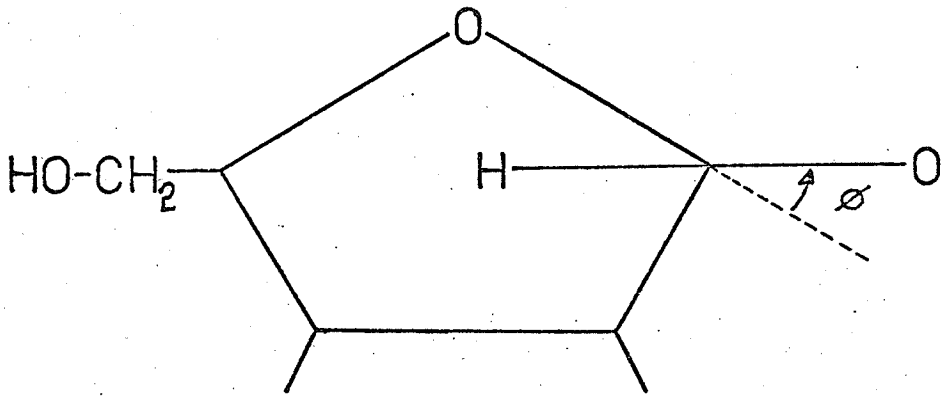

$\phi_{CN} \cong -50°$

ANTI - CONFORMATION

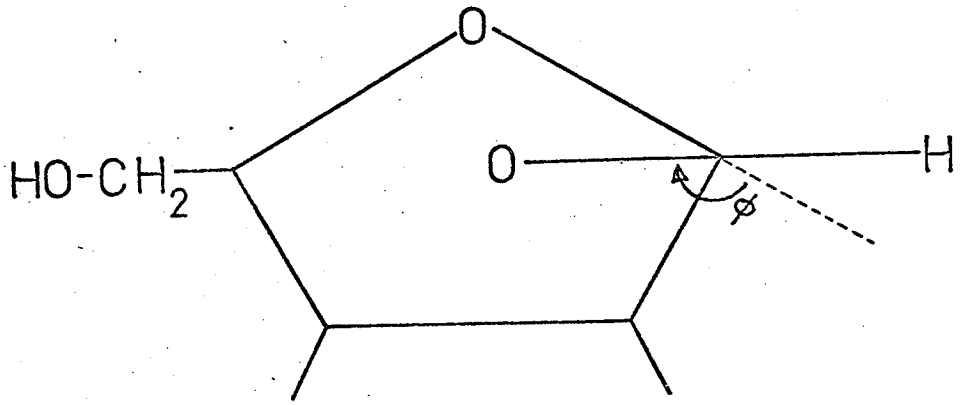

$\phi_{CN} \cong 130°$

SYN - CONFORMATION

CHAPTER III

A Brief Review of Nuclear Magnetic Resonance Applied to Conformational Studies

A. Introduction

A wide variety of techniques have been used to study nucleic acids, including UV, IR, CD, ORD, X-ray, and NMR spectroscopy. UV and IR are best suited to studies of inter- and intra-molecular hydrogen bonding, determination of tautomeric structure, and investigations of intact polynucleotides in which the helix-coil transitions are marked by distinct changes in UV absorbance. Optical rotation and circular dichroism reflect the degree of symmetry or asymmetry, such as the intrinsic asymmetry of sugars or the asymmetric arrangement of chromophores in a helix. Several groups of workers, notably those of Ulbricht[91,92], and Miles et al.[93] have noted that ORD and CD changes can also be correlated with the sugar-base torsion angle, ϕ_{CN}. X-ray studies produce detailed conformational data, giving all bond lengths, angles, and relative positions, but these studies must be carried out on the crystalline state. While the conformation of a molecule in the crystal lattice often corresponds to the preferred conformation in solution, it is dangerous to extrapolate without additional evidence. The inter-molecular distances in solution are significantly greater than in a crystal, so interactions such as hydrogen bonding or base "stacking" may become less important, especially in dilute solutions. For example, 4-thio-uridine was shown to exist as the syn conformer in the

crystal[94], and as the anti conformer in solution[95].

By comparison NMR is capable of studying nucleosides and nucleotides in aqueous solutions that are sufficiently dilute to minimize intermolecular interactions. The majority of studies have been done on monomer units, as these provide readily interpreted spectra, however progress is being made in the application of NMR to polynucleotides and intact nucleic acids[24]. NMR also provides values for several independent parameters, the shifts and coupling constants, which have recognized relationships to various structural and electronic features.

B. Factors Affecting the Chemical Shift

The resonance condition for a nucleus in a magnetic field B_o is given by the equation:

$$\nu_i = |\gamma_i/2\pi| \; B_o \; (1-\sigma_i)$$

where ν_i, γ_i, and σ_i are the resonance frequency, magnetogyric ratio, and shielding constant respectively, for a nucleus i. Thus variations in σ_i will cause variations in resonance frequencies. The screening term σ_i can be broken down into several parts which are somewhat arbitrary but quite useful.

$$\sigma = \sigma_d(\text{local}) + \sigma_p(\text{local}) + \sigma_m + \sigma_r + \sigma_e + \sigma_s$$

where

$\sigma_d(\text{local})$ = local diamagnetic term

$\sigma_p(\text{local})$ = local paramagnetic term

σ_m = neighbour anisotropy effect

σ_r = ring current effects

σ_e = electric field effects

σ_s = solvent (or medium) effects

The local diamagnetic term arises from the circulation of electrons induced by B_o, producing a secondary field at the center of motion which opposes B_o and gives a lower resonance frequency. The presence of electronegative substituents reduces electron density around the nucleus, decreasing the shielding effect due to $\sigma_d(\text{local})$.

The presence of other nuclei around the magnetic nucleus hinders the diamagnetic circulation of electrons, reducing σ_d. The contribution is known as the paramagnetic term, and may become large if there is an asymmetric distribution of p or d orbitals near the nucleus, or if there are low-lying excited states which may be mixed in by interaction with B_o, producing an asymmetric charge distribution. It is generally accepted that the paramagnetic term is not the dominant one for protons.

The magnetic moment induced by the external field in a group of orbitals may in some circumstances contribute to the shielding of a distant proton. If the induced moment is isotropic, i.e. its magnitude and direction independent of orientation with respect to the external field, then the effect on a distant proton will be averaged to zero by the rapid tumbling of the molecules. If however the induced moment is anisotropic there may be a net shielding or deshielding effect[104, 81-85]. Figure 8 shows the nodal cones of shielding[104] for the C=O and C=C groups. This is known as the neighbouring group anisotropy effect, σ_m.

Ring current effects, σ_r, are thought to arise when an aromatic ring is perpendicular to the applied field B_o. The field causes a diamagnetic circulation of the π electrons giving rise to a field which opposes B_o at the center and reinforces it at the periphery.

Figure 8

Schematic representation of the nodal cones of shielding for C=O and C=C. The positive and negative signs refer to the effect on the shielding constant (σ) of a distant nucleus. (Ref. 104,p.89).

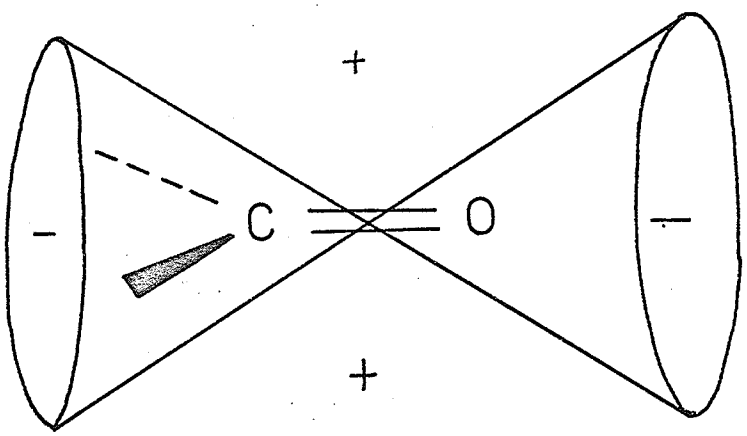
+
C
O
−
−
+

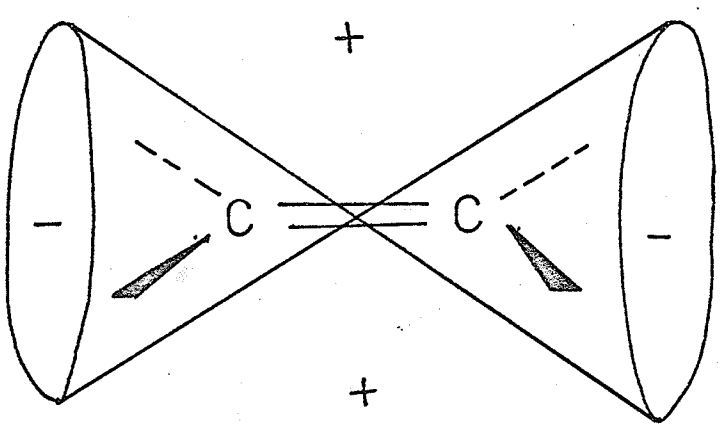
+
C
C
−
−
+

Thus the protons in benzene experience a shift to low field. While this concept has been criticized, notably by Musher[43] who prefers to consider it the sum of local contributions, the ring current provides a semi-quantitative understanding of the contribution of σ_r to the total shielding constant.

Polar groups in a molecule distort the electron density in the rest of the molecule, giving rise to the electric field shielding, σ_e. There are two contributions to σ_e.

$$\sigma_e = -AE_z - BE^2$$

where A and B are constants, and z is the direction of the bond affected, from the C to the H. The first term is due to the drift of electrons caused by the electric field E. The second term is due to the distortion of the electron density around the nucleus, and is thus a paramagnetic contribution. Normally the E_z term is dominant for protons. The effect is shown schematically in Figure 9, in which the electrons drift against the direction of E, shielding the proton.

The solvent, or medium, in which the sample is studied can affect the molecule by the same sort of mechanisms as have been described above. As a result the term σ_s can be further divided into five separate terms.

Figure 9

Schematic representation of the electric field shielding for C=O. The electrons in the C-H bond drift against the direction of the field E caused by the C=O, shielding the proton. (Ref.104,p.93)

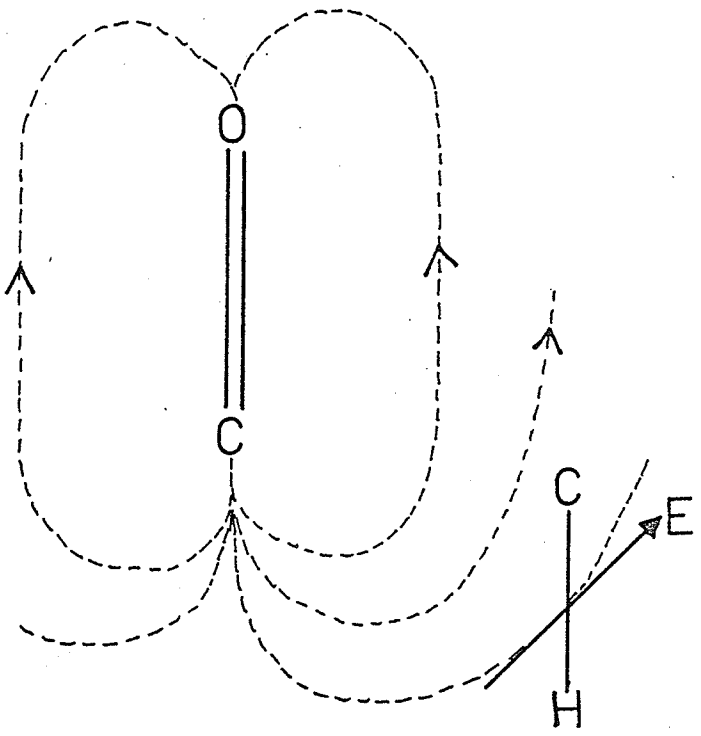
O
C
C
E
H

$$\sigma_s = \sigma_B + \sigma_W + \sigma_a + \sigma_E + \sigma_c$$

These are, in the above order, bulk magnetic susceptibility effects, van der Waal interactions, solvent diamagnetic anisotropy, electric polarization and polarizability of the solvent, and complex formation due to weak effects such as hydrogen-bonding and charge transfer. These effects are discussed in some detail by Jackman and Sternhell[44] and will not be covered further here, except to note that where an internal reference is used, only the differences in these effects on the solute and the standard are measured.

Hydrogen bonding is mentioned above between solvent and solute, but there is also the possibility of intramolecular hydrogen bonding or intermolecular solute-solute hydrogen bonding. For strong hydrogen bonds, the dominant effect is likely the electrostatic effect of the donor, for weaker bonds, the diamagnetic anisotropy of the donor. In both cases the resonant frequency of the proton is usually shifted to low field by formation of the hydrogen bond[104].

C. Spin-Spin Coupling Constants and Structure

Spin-spin coupling is highly structure-dependent, offering a powerful tool for structural studies. The theory of spin-spin coupling is rather complex. It is reviewed in some detail by Jackman and Sternhell[45], and by Bovey[46]. There is considerable empirical data relating the spin-spin coupling constant (J) to structural features, some of which are now supported by theoretical calculations. Following the approach of Sternhell[47], some of these correlations are discussed below. Only those correlations which are applicable to the nucleosides under consideration are discussed here. The review by Sternhell is much broader in scope.

1. Geminal Coupling

Geminal coupling constants (Jgem) across an sp^3 hybridized carbon atom can take up a wide range of values, from -22 Hz to + 6 Hz. The effect of substituents on the sp^3 carbon has been rationalized in terms of inductive electron withdrawal producing a positive increment to Jgem and hyperconjugative electron withdrawal producing a negative increment. The hyperconjugative effect is more strongly conformation-dependent.

Electronegative α -substituents produce an inductive withdrawal, and hence a positive increment to Jgem. These effects are approximately additive if the

groups are freely rotating or have identical orientations. Conversely, if the α-substituent possesses lone pairs, the "eclipsing effect" of the lone pairs with the C-H bonds of the methylene groups are strongly orientation-dependent. For O,N, and S the effect is about +2 to +3Hz. These lone pair effects are superimposed on the positive increments due to inductive withdrawal, leading to a conformational dependence of Jgem in some cases. β - substituents produce a negative increment in Jgem with increasing electronegativity. The relationship is more complex than for the α-substituents and appears to depend upon orientation.

2. Vicinal Coupling

Vicinal coupling is that between nuclei separated by three bonds. For the fragment H_A-C-C-H_B, the values of $^3J_{AB}$ commonly range from -0.3Hz to +14Hz. The magnitude of $^3J_{AB}$ is related to the dihedral angle Ø (defined in Figure 10). The relation was given a quantitative expression by Karplus[48,49] in the form:

$$J = J^{\circ} \cos^2 \phi - C \quad \text{for} \quad 0^{\circ} \leq \phi \leq 90^{\circ}$$

$$J = J^{180} \cos^2 \phi - C \quad \text{for} \quad 90^{\circ} \leq \phi \leq 180^{\circ}$$

The original calculated values for the constants were J°= 8.5 Hz, J^{180}= 9.5 Hz, and C= -0.3Hz, for an unsubstituted ethanic fragment. Alternative formulations

have since been offered[49], but the original expressions have been found to be qualitatively quite successful in a large number of molecules despite their limitations. The most widely used modification is the substitution of different values for J^0 and J^{180} to fit the data for groups of compounds having distinct structural similarities. Several sample curves for selected values of J^0 and J^{180} are shown in Figure 10. By using Dreiding models to select the more probable conformations, then using the Karplus relations to select from these possibilities, it is possible to solve the majority of conformational problems.

In view of the numerous effects on J_{vic}, values of J^0 and J^{180} should only be chosen from comparisons with closely-related systems. In a later paper[49], Karplus cautions against using the dihedral angle relation without due allowance for effects of substituents, different bond angles and bond lengths. In the system H_A-C_1-C_2-H_B, if the stereochemistry remains unchanged, the addition of an electronegative substituent to C_1 or C_2 tends to lower the value of J_{AB}. The maximum effect seems to occur when the substituent is attached by a bond <u>trans</u> to one of the protons. Conversely, a lone pair of a heteroatom contributes a positive increment to J_{vic} amounting to +2.3 Hz when the lone pair and the carbon-hydrogen bond are perfectly eclipsed. If the electronegative substituent is one carbon atom removed from the coupling

Figure 10

Plot of the Karplus relation for selected values of J^{o} and J^{180}. (Ref. 47,p.247)

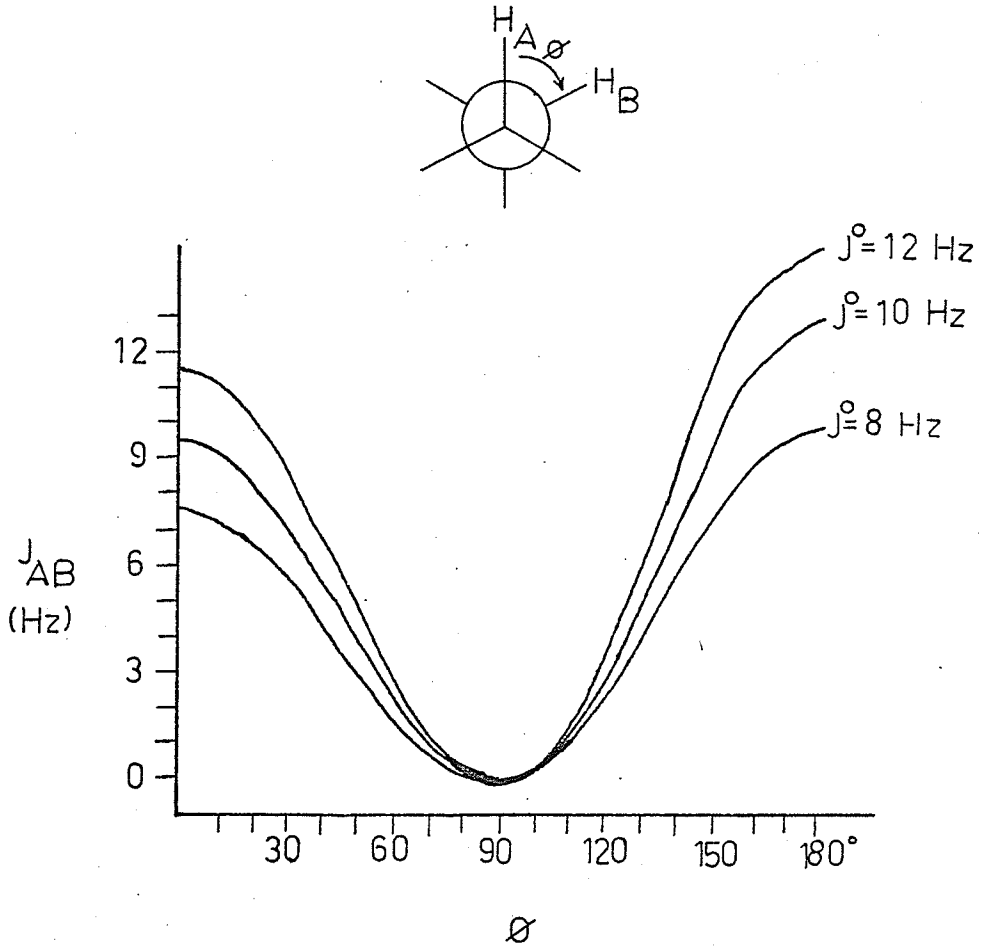
H_A
ø
H_B
J°= 12 Hz
J°= 10 Hz
J°= 8 Hz
J_AB
(Hz)
12
9
6
3
0
30
60
90
120
150
180°
ø

path, it causes an increase in J_{AB}, and there are indications that the trend reverses again if the electronegative substituent is removed one more carbon away[50].

Vicinal coupling in $H_A-C=C-H_B$ is correlated with the nature of the substituents, ring size in cyclic compounds, and with the cis-trans relation between H_A and H_B. In general J_{vic} gets smaller as the sum of the electronegativities of the substituents increases. A more definite assignment can be made by comparison with some of the published data[51,52,53]. There is evidence that this effect is also reversed when the substituent is removed by an extra bond, i.e.

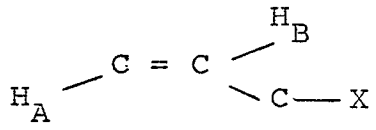

Vicinal J's show a marked decrease as the ring size decreases, both in simple cyclic alkenes and non-aromatic cyclic polyenes. Moreover, introduction of a heteroatom into the ring adjacent to the double bond causes a further decrease in J_{vic}.

In virtually all cases, it is found that J_{cis} is smaller than J_{trans}, providing none of the other factors are altered in changing the conformation about the double bond.

3. Long-Range Coupling

Long-range J's are usually of the order 0-2.5 Hz, and both experimental data and theoretical and semi-empirical considerations suggest that there are certain prefered bond orientations. For four bonds, the most favourable path is the planar zig-zag, or 'W', arrangement. This is independent of the nature of hybridization of the intervening atoms. The mechanism is thought to involve only the σ electrons, and the magnitude falls off rapidly as the system loses coplanarity. The 'W' coupling is positive in completely saturated systems, although some non-coplanar geometries have produced small negative J values[53]. A theoretical study by Barfield[55] indicates that while the sign of the coupling constant is positive for the planar 'W' configuration, this is true for only a very small range of values for ϕ and ϕ' (see Figure 11) around $\phi=\phi'=180^{\circ}$. For most other values, the coupling constant is calculated to be negative. Barfield's data is given in Table I. These values were calculated for three sp_3 hybridized carbons, and do not necessarily cover cases where the center C is sp_2 hybridized (H-C-C-C-H). One example is the study by Lazlo and Musher[54], where the axial protons in the system:

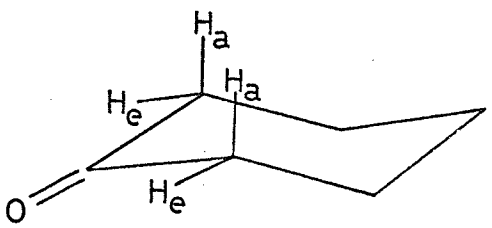

Figure 11

Specification of the dihedral angles Ø and Ø' (Ref.55). Both angles are measured clockwise from the C_1-C_2-C_3 plane.

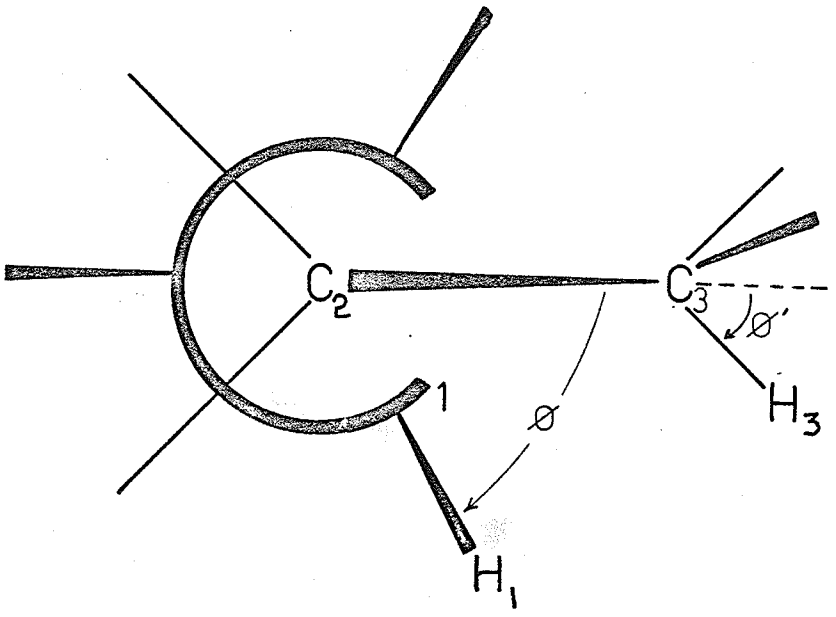
C2
C3
1
H1
H3
ø
ø'

TABLE I

Calculated INDO* Results for $^4J_{HH'}$ in Propane[55]

ø' deg	ø' deg	$^4J_{HH'}$ Hz	ø' deg	ø' deg	$^4J_{HH'}$ Hz
0	0	-1.04	120	120	-0.12
	60	-0.58		180	+0.45
	120	-0.25		240	-0.29
	180	-0.29		300	-0.62
	240	-0.25	180	180	+1.44
	300	-0.58		240	+0.45
60	60	-0.71		300	-0.49
	120	-0.46	240	240	-0.12
	180	-0.49		300	-0.46
	240	-0.62	300	300	-0.71
	300	-0.32			

* Intermediate Neglect of Differential Overlap

have a positive coupling of 1.0-1.3 Hz. Barfield predicts $J \cong -.7$ Hz for this orientation; $\emptyset=\emptyset'=300^{o}$, when all carbons are sp^3 hybridized.

An "extended W' path of five bonds also appears to be a favourable arrangement, with observed J's of the order 0.6-1.0 Hz, as long as the path is planar[56].

These factors must all be considered when attempting to reconcile the observed spectrum with any proposed molecular structure.

CHAPTER IV

Experimental

The 2,2'-anhydrouridine was prepared by D.Iwacha and K.K.Ogilvie at the University of Manitoba; the arabinouridine was obtained from Terra-Marine Bioresearch, California; and the internal reference, 3-trimethylsilyl propane sulfonic acid, sodium salt (DSS) was a product of E.Merck, Germany. All were used without further purification. Two sets of samples were prepared, one set for the Varian HA-100D nuclear magnetic resonance spectrometer at the University of Manitoba, and one set for the Varian HR-220 proton magnetic resonance spectrometer at the Ontario Research Foundation, Sheridan Park, Ontario. The concentrations for the 100MHz instrument were as follows:

0.29 M arabinouridine/0.15 M DSS; and
0.23 M anhydrouridine/0.18 M DSS.

The 220MHz instrument required less concentrated samples, the ones used being 0.14 M arabinouridine/0.06 M DSS; and 0.07 M anhydrouridine/0.06 M DSS. The spectrum of cU was found to be virtually independent of concentration effects up to the concentration used while aU showed a change in shifts of the H_1, and H_2, regions of ~2 Hz from 0.2M to 0.3M. No change in coupling constants was noted for either compound. These effects are not felt to be significant. The pD was adjusted to neutrality (pD=pH+0.40)[58] with small amounts

of dilute DCl or NaOD. The samples were lyophilized three times with D_2O to reduce the size of the HDO signal, which occurs very near to the H_3, signal at 30°C.

The 220MHz spectra were used for the initial analysis, as the difference in the H_4' and H_5' shifts is small at 100MHz, especially in arabinouridine. The computer simulations were fit to the 100MHz spectra, as these could be calibrated more accurately.

All 100MHz spectra were run on a varian HA-100D nuclear magnetic resonance spectrometer operating in the frequency sweep mode. Peaks were calibrated by interpolation from calibration lines which were measured relative to the internal lock signal by counting the sweep oscillator frequency to the nearest 0.01 Hz. All 100MHz spectra were recorded at a frequency sweep rate of 0.02 Hz/second.

The high and low temperature studies were carried out using the V-4341/V-6057 variable temperature accessory. Temperatures are accurate to within $\pm$2.0°C.

The accuracy with which chemical shifts could be measured was a function of the linewidth. Despite the broadening observed at lower temperatures, all shifts are considered accurate to $\pm$0.1 Hz.

The spectra were analyzed with the aid of a LAOCN3 program[96,97] modified by R.Wasylishen for the IBM 360/65 computer. The computed spectral curves were produced by

a CALCOMP 750/563 incremental pen plotter using data from LAOCN3.

CHAPTER V

Results and Discussion

A. Arabinouridine

1. Spectral Assignment

The observed spectra of arabinouridine at 5°C, 30°C, and 80°C are shown in Figures 12-14, each accompanied by the computer-simulated spectrum. The proton chemical shifts and coupling constants for aU at all three temperatures are shown in Table II, with the values for uridine at 28°C [59]. The shifts for uridine were found to be virtually independent of temperature from 28°C to 78°C [59]. Those for aU vary less than 1.0 Hz from 5°C to 80°C except for H_1' and H_6 which change 2.8 Hz and 6.3 Hz respectively. Comparison of the spectra reveals improved resolution at the higher temperatures. For this reason, the following discussion considers the values of the shifts taken from the spectrum at 80°C, as typical values, changes in H_1' and H_6 being discussed separately.

The initial assignments were made by comparison with uridine. The doublet at 7.802ppm is assigned to the H_6 proton of the pyrimidine base, as C_6 is adjacent to a nitogen atom. The resonance at 5.857ppm is a doublet with the same splitting as H_6 and consequently was assigned to the H_5 proton. Additional support for these assignments comes from the presence of two small couplings, $J_{1'5}$ and $J_{1'6}$. Their presence was verified by decoupling experiments, however they do not appear

Figure 12

The 100MHz spectrum of arabinouridine at 5°C with the scale in PPM to low field of DSS. The lower spectrum is the experimental one, while the upper is a computer-fitted simulation.

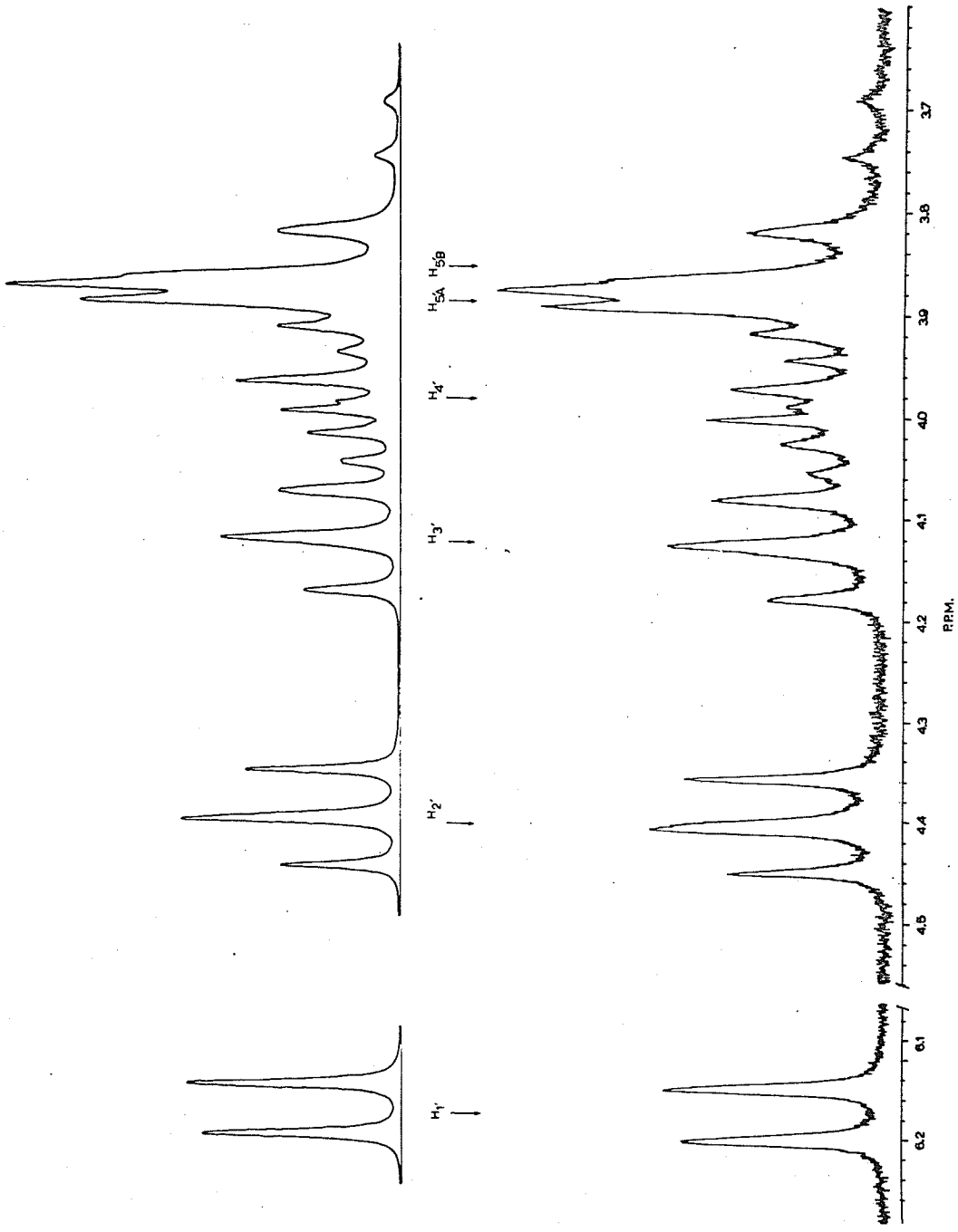
H1'
H2'
H3'
H4'
H5A
H5B
6.2
6.1
4.5
4.4
4.3
4.2
4.1
4.0
3.9
3.8
3.7
P.P.M.

Figure 13

The 100MHz spectrum of arabinouridine at 30°C with the scale in PPM to low field of DSS. The lower spectrum is the experimental one, while the upper is a computer-fitted simulation.

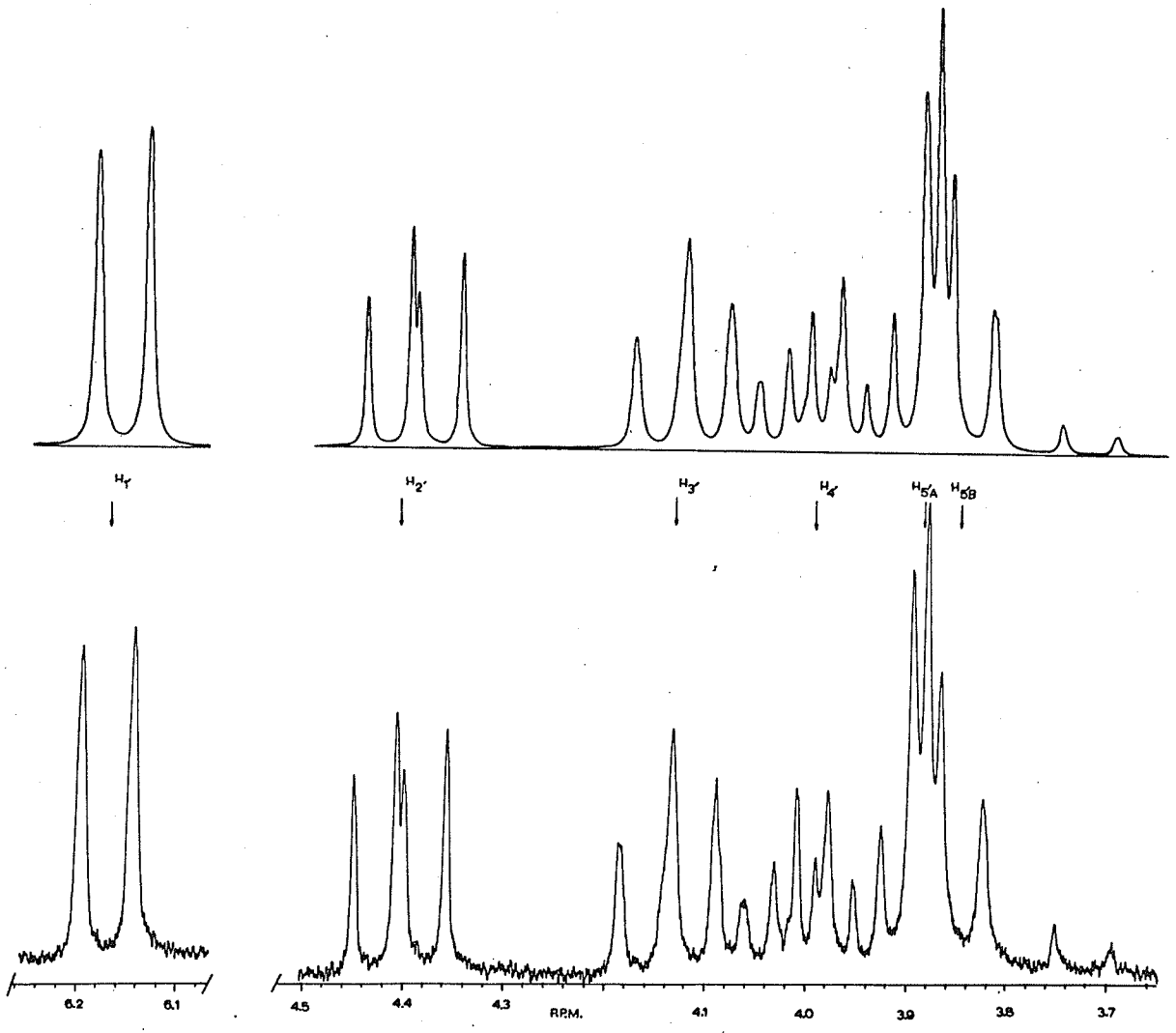
H1'
H2'
H3'
H4'
H5'A
H5'B
6.2
6.1
4.5
4.4
4.3
R.P.M.
4.1
4.0
3.9
3.8
3.7

Figure 14

The 100MHz spectrum of arabinouridine at 80°C with the scale in PPM to low field of DSS. The lower spectrum is the experimental one, while the upper is a computer-fitted simulation.

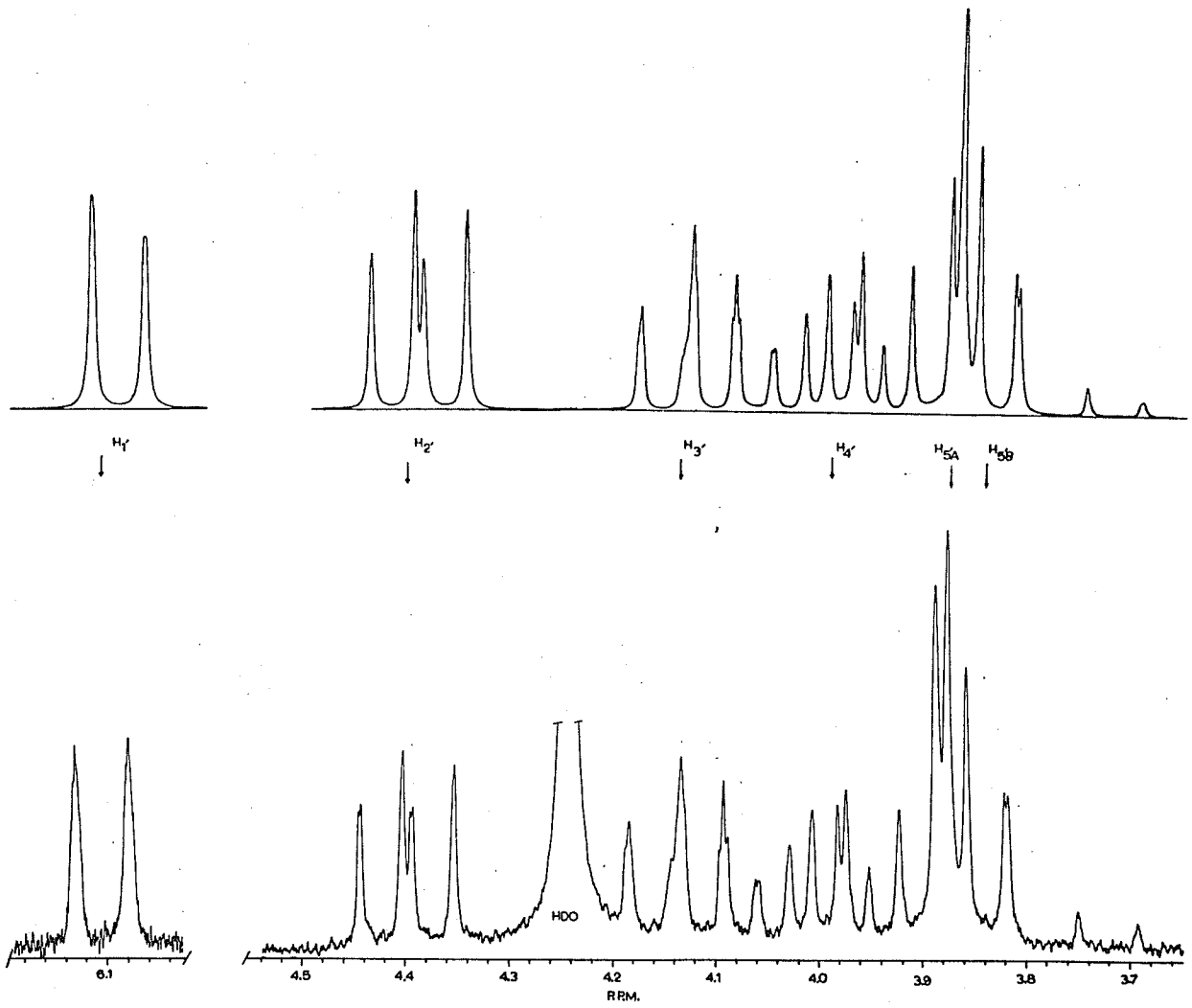
H1'
H2'
H3'
H4'
H5'A
H5'B
HDO
6.1
4.5
4.4
4.3
4.2
4.1
4.0
3.9
3.8
3.7
P.P.M.

Table II

	aU 5°	aU 30°	Uridine 28°	aU 80°
H_6	7.865	7.839	7.862	7.802
H_5	5.851	5.860	5.887	5.857
H_1'	6.175	6.169	5.901	6.147
H_2'	4.400	4.398	4.341	4.396
H_3'	4.124	4.128	4.222	4.133
H_4'	3.983	3.988	4.128	3.987
$H_5'_A$	3.911	3.907	3.907	3.902
$H_5'_B$	3.827	3.827	3.803	3.829
$J_{1'2'}$	5.11	5.11	4.4	5.10
$J_{1'3'}$	(0.30)	(0.30)	-	(0.30)
$J_{1'5}$	-	-	-	0.41
$J_{1'6}$	-	-	-	0.14
$J_{2'3'}$	4.72	4.53	5.3	4.33
$J_{3'4'}$	5.71	5.53	5.5	5.44
$J_{3'5'A}$	(-0.15)	(-0.15)	-	(-0.15)
$J_{3'5'B}$	(-0.15)	(-0.15)	-	(-0.15)
$J_{4'5'A}$	3.05	3.23	3.0	3.41
$J_{4'5'B}$	5.47	5.55	4.4	5.51
$J_{5'A\ 5'B}$	-12.64	-12.49	-12.7	-12.40
J_{56}	8.15	8.10	8.0	8.15

in the H_1' region of the simulated spectrum as LAOCN3 is not capable of handling eight spins.

The H_1' proton appears as a doublet centered at 6.147 ppm. The broadness of the peaks is due to multiple long-range or virtual couplings, and possibly quadrupolar broadening by the adjacent N_1 nitrogen atom.

The H_4', $H_5'_A$, and $H_5'_B$ resonances form a characteristic ABC pattern with H_4' centered at 4.133 ppm; $H_5'_A$ and $H_5'_B$ at 3.902 and 3.829 ppm repectively. No reasonable assignment of the 5'-methylene hydrogens could be made here although some workers[86,87] have attempted assignment in other instances. H_2' and H_3' were assigned by comparing vicinal couplings and verified by double irradiation experiments.

The calculated spectra shown in Figures 12-14 simulate the 1'-5' regions satisfactorily in all three cases.

The base protons in aU are shifted ~ 0.025 H_z upfield with respect to those in uridine. This can be attributed to the change in position of the 2'-OH, so that it is now *cis* to the H_5 and H_6. Ts'o *et al.*[62], and Gatlin and Davis[63], have pointed out that the "*cis*-OH" effect is a magnetic one rather than inductive, and consequently it is quite capable of acting through space in this manner. Supporting this hypothesis is the downfield shift of H_1' in aU (0.246 ppm) which would

correspond to the loss of the expected shielding contribution of a cis-OH. The difference in the size of the effects can be attributed to the differences in the O-H_1' and O-H_5, O-H_6 distances. It is interesting that of these three, H_1' and H_6 exhibit the strongest temperature dependence. The trend is for increased shielding of both with increasing temperature. If the sugar-base torsion angle was changing in such a way as to bring the 2'-OH nearer to the H_6 atom, the C_2 oxygen would also move closer to H_1', causing a shielding of H_1' by the anisotropy of the C=O bond.

The change in the H_2' shift is less easily explained. As it has moved cis to the 3'-OH it should also move upfield, however the observed change is 0.043 ppm downfield. One possible explanation is that the H_2' in uridine may be shielded by the anisotropic C=C of the heterocyclic ring and the loss of this shielding is not completely compensated for by the gain of the cis-OH, leaving a net deshielding effect.

The H_3' resonance also shows the gain of a cis-OH in an upfield shift of 0.089 ppm.

The H_4' signal is shifted 0.141 ppm to high field, indicating an increase in shielding. It is unlikely that the different position of the 2'-OH would have a direct effect at this distance. Other workers have noted similar effects, but no satisfactory explanation of the H_4' shift has been proposed.

The shifts of the H_5' protons are found to be virtually identical to those in uridine. It would be convenient to dismiss this section by saying that this similarity indicated identical environments in both molecules. However, it is suggested in section 5 that the rotamer populations have changed in such a way that the protons are spending more time above the sugar ring. This would bring them into closer contact with the 2'-OH, and with the anisotropic C=C of the heterocyclic ring. Therefore this similarity of shifts for H_5' in aU and U is probably somewhat coincidental being the net result of several opposite effects rather than a result of identical environments.

2. Anomeric Configuration

The use of H_1' shifts to establish the anomeric configuration has met with some success[64,65], while application of the Karplus relation to $J_{1'2'}$ to determine the 1' 2' dihedral angle is thought to be much less satisfactory[4]. Lemieux and Lineback[66] suggest that in view of the limitations of the Karplus relation and the dihedral angles involved here, anomeric configuration should only be assigned from the vicinal coupling when the value of $J_{1'2'}$ is less than 1 Hz. Since the value for aU is 5 Hz, assignment of the anomeric configuration by the Karplus relation was not attempted.

As was pointed out in the previous section, the presence of a cis-OH group causes a shielding effect due to the proximity of the oxygen atom. It has been noted[4] that observed differences in the H_1' shift for anomeric pairs of a variety of furanosides could be accounted for by the change in proximity of the 2'-OH group. By comparison to uridine[4], and allowing for the change in position of the 2'-OH, it is apparent that the compound studied should be the β-anomer (Figure 15).

3. The Sugar-Base Torsion Angle

The sugar base torsion angle (ϕ_{CN}) was defined by Donohue and Trueblood[77] to describe the orientation of the base and sugar ring about the glycosidic bond. The two isomers usually considered for nucleosides have the syn or anti conformation, as shown in Figure 16. The majority of pyrimidine nucleosides studied to date have been shown, by NMR, ORD, and X-ray studies, to have the anti conformation in aqueous solution. One of the few exceptions is orotidine, which possesses a bulky carboxyl at the C_6 position of the base. The steric interactions between the carboxyl group and the sugar cause the base to exist preferentially in the syn conformation with the smaller C_2 keto group positioned over the sugar[78].

Figure 15

Schematic illustrations of the α- and β- anomers of arabinouridine.

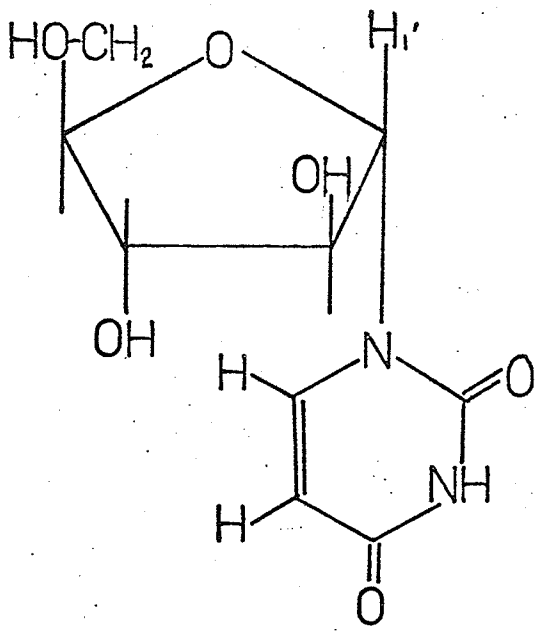

α- aU

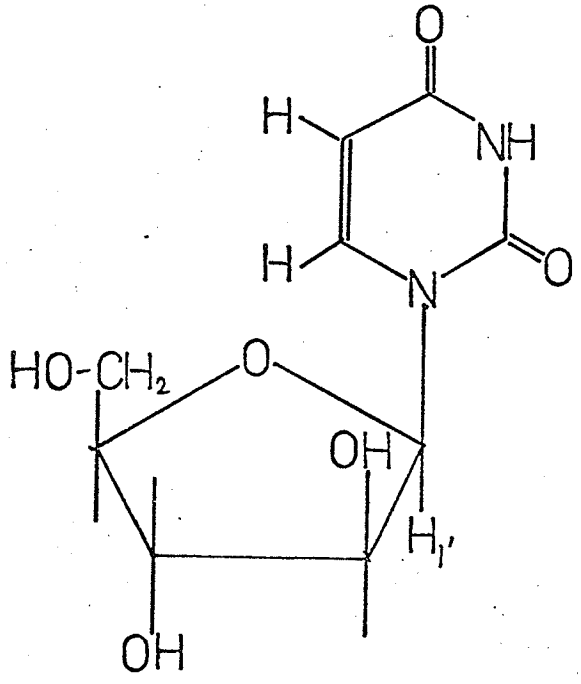

β - aU

Figure 16

SYN and ANTI configurations of aU showing approximate values for the sugar-base torsion angle ϕ_{CN}.

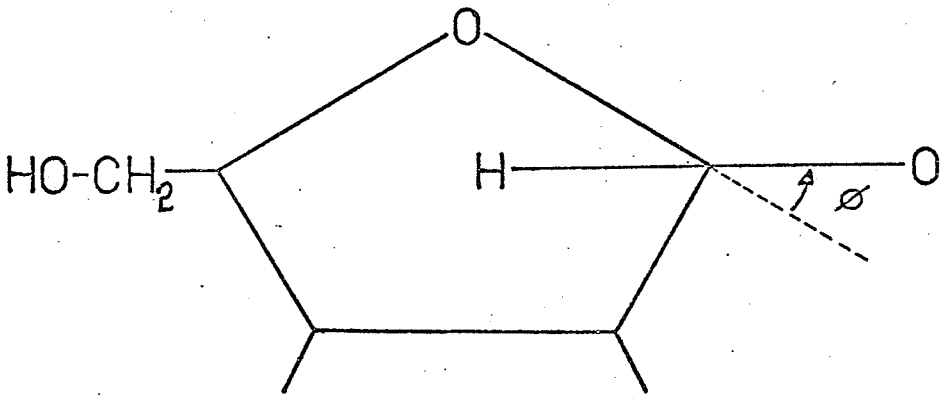

$\phi_{CN} \cong -50°$

ANTI - CONFORMATION

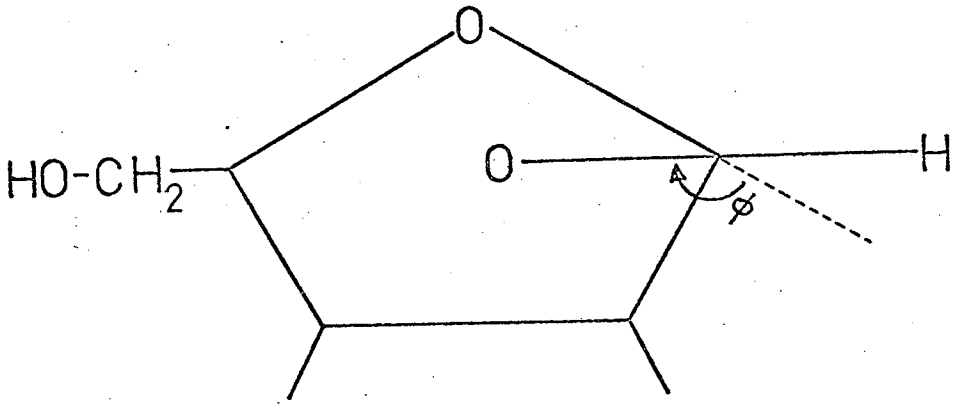

$\phi_{CN} \cong 130°$

SYN - CONFORMATION

Uridine has been shown to exist in the anti conformation in aqueous solution[59]. Comparison of space-filling models of uridine and aU indicate similar steric considerations must apply to both, so aU is expected to exist in the anti conformation also.

Support for the choice of the anti conformation comes from the existance of the long-range coupling $^5J_{1'5}$ observed at 80°C. The most favourable stero-chemistry for coupling over five bonds is the planar, extended"zig-zag" path. This path connects H_5 and $H_{1'}$ in the anti, but not in the syn conformation, and the existance of such a coupling has been suggested as evidence that the anti is the prefered conformation[98]. Optical studies by Guschlbauer and Privat de Garilhe[14] and Miles et al.[99] on aU, and an X-ray study by Tougard[103] on 5-Br-aU, indicate that the anti conformation is prefered both in solution and in the crystalline form.

Comparison of ribose proton shifts for syn nucleosides with those of nucleosides known to exist in the anti conformation has shown that $C_{1'}$, $C_{2'}$, and $C_{3'}$ are appreciably deshielded if the molecule is syn[79]. However the change in the position of the 2'-OH in aU alters the chemical shifts in such a manner that any comparison to other anti nucleosides such as uridine produces ambiguous results, preventing their use in

determining the torsion angle.

The signs of $^{5}J_{1'5'}$ and $^{4}J_{1'6}$ were not determined, but their magnitudes are .41 H_z and .14 H_z respectively. The larger value of $J_{1'5}$ despite the extra bond, can be attributed to the extended "zig-zag" path from $H_{1'}$ to H_5. The 'W' path does not exist for $^{4}J_{1'6}$ but a small non-zero coupling is predicted for this path also[100].

These couplings are seldom observed in other nucleosides since they are highly sensitive to the conformation about the N-glycosyl bond.

Gushlbauer and Privat de Garilhe[14] suggest that the 2'-hydroxyl in aU restricts the rotation about the N-glycosyl bond to a narrow range of angles about the anti position. This is consistent with the observation of a larger value of $J_{1'5}$ than occurs in uridine since this long-range coupling is expected to increase with the percentage of anti conformer.

4. Conformation of the Furanose Ring

The Karplus relation has been used extensively to determine the geometry of ring systems[4,59,67-71]. The technique must be applied with considerable caution however, as the Karplus relation was never intended for anything more accurate than an indication of the probable range of Ø values[49]. The basic approach

may be exemplified by the work of Hall et al.[67] as applied to aU below.

Hall and his coworkers, notably Paul Steiner, have developed a treatment for cyclopentane rings based on the following assumptions:

i. All the ring carbons possess precise tetrahedral symmetry.

ii. Only "envelope" (C_S) and "twist" (C_2) conformations are considered. The twist conformer ${}^{m}T_{n}$ having atom m endo, and atom n exo with reference to the remaining three atoms; while the envelope conformer V_n, or ${}^{n}V$, has atom n exo, or endo, respectively with reference to the other four atoms. (For nucleosides, endo is defined as being on the same side of the reference plane as the C_4'-C_5' bond, exo is on the opposite side.)

iii. "Maximal" puckering always occurs, so that the envelope conformation resembles one end of a cyclohexane "chair" form.

For furanose sugars, to which they have extended this method, there are thus twenty possible conformations. These are represented by the CYCLE Of PSeudorotation (CYCLOPS) shown in Figure 17.

The coupling constants of interest are $J_{1'2'}$, $J_{2'3'}$, and $J_{3'4'}$. Applying the Karplus relation, the approximate values for $\phi_{1'2'}$, $\phi_{2'3'}$, and $\phi_{3'4'}$ may be

Figure 17

CYCLE Of PSeudorotation (CYCLOPS)[67] giving the possible conformations of the furanose ring. The two conformations indicated by this scheme for aU are illustrated below.

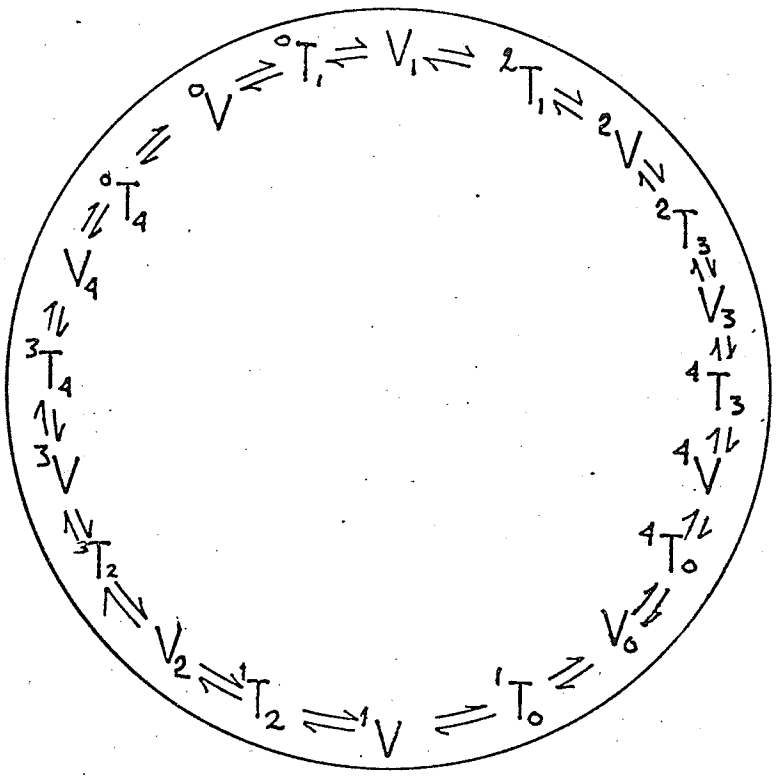
°V ⇌ °T₁ ⇌ V₁ ⇌ ²T₁ ⇌ ²V ⇌ ²T₃ ⇌ V₃ ⇌ ⁴T₃ ⇌ ⁴V ⇌ ⁴T₀ ⇌ V₀ ⇌ ¹T₀ ⇌ ¹V ⇌ ¹T₂ ⇌ V₂ ⇌ ³T₂ ⇌ ³V ⇌ ³T₄ ⇌ V₄ ⇌ °T₄

CYCLOPS

°V ≡

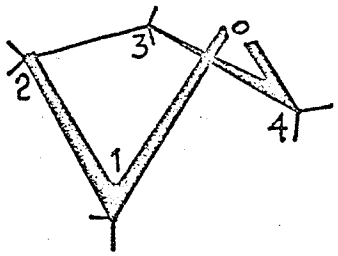
3
0
2
4
1

¹V ≡

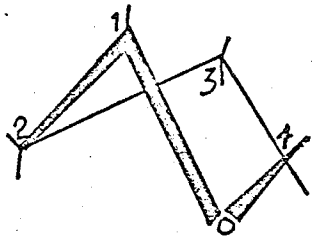
1
3
2
4
0

calculated. The values of J° chosen are those suggested by Abraham *et al.*[72] for several carbohydrate ring systems:

$$J^{0}=9.27,\ 0 \leq \phi \leq 90^{\circ},\ J^{180}=10.36,\ 90^{\circ} \leq \phi \leq =180^{\circ}$$

The calculated dihedral angles are shown in Table IIIa. It is then necessary to compare these values to those shown in Table IIIb. The majority of the conformations may be eliminated as having one or more angles deviating widely from the calculated values. The conformations whose values form the closest fit to the calculated ø's are ^{1}V and ^{0}V. The ^{0}V values are the best, and this is the most reasonable form on steric grounds as well. With the oxygen atom in the *endo* position, the $-CH_2OH$ and base ring are at the maximum separation. In addition, the distance between the 2'-OH and the base has increased almost to that of the V_2 conformation, which offers the maximum possible. ^{0}V could be a compromise between these two considerations.

Hruska *et al.*[4] use basically the same approach, but employ different values for the dihedral angles of the various ring conformations. They also use only the limiting *exo* and *endo* cases, ignoring the intermediate "twist" conformers.

Both authors state that their values of ϕ_{ij} for each conformation were measured from Dreiding models, yet their published values[67,4] vary by as much as 30°

Table III

a) Calculated Dihedral Angles for the aU Furanose Ring

Temp.($^{\circ}$C)	$J_{1'2'}$	$\phi_{1'2'}$	$J_{2'3'}$	$\phi_{2'3'}$	$J_{3'4'}$	$\phi_{3'4'}$
5°	5.0	41.0	4.7	133.9	5.7	139.4
30°	5.1	40.4	4.5	132.8	5.5	138.3
80°	5.1	40.4	4.3	131.7	5.4	136.8

continued...

Table III - continued

b) Dihedral Angles for the Conformations of CYCLOPS

Conform	Ø12'	Ø23'	Ø34'
^{o}V	30	120	150
$^{o}T_1$	50	90 X	150
V_1	50	90 X	120
$^{2}T_1$	60	70 X	100
^{2}V	50	70 X	90
$^{2}T_3$	50	60 X	90
V_3	30	70 X	70
$^{4}T_3$	20	70 X	60
^{4}V	0	150	70 X
$^{4}T_o$	20	100	50 X
V_o	30	120	90 X
$^{1}T_o$	50	140	100 X
^{1}V	50	150	120
$^{1}T_2$	60	170 X	140
V_2	50	170 X	150
$^{3}T_2$	50	180 X	170
^{3}V	30	170 X	170
$^{3}T_4$	20	170 X	180
V_4	0	150	170 X
$^{o}T_4$	20	140	170 X

X - indicates parameter with the greatest deviation from the experimental values.

(for the C_2' *exo* form). The work of Abraham and McLauchlan[68] offers the basis of an explanation of this variation. These authors show that it is possible to have a wide range of dihedral angles for one conformation, depending upon the extent to which the ring is buckled. For example, it is possible to maintain approximate tetrahedral symmetry for all ring atoms in the envelope conformation with the single atom bent from 0° to 50° out of the plane. Hall *et al.* specify "maximal" puckering, while Hruska *et al.* make no reference to this point, so it is quite reasonable that slightly different values of Ø should appear.

According to the CYCLOPS scheme, the most probable conformation for the furanose ring in aU is thus the ^{0}V, or O-*endo* form. It is worth repeating here an observation of Hall and Steiner[67,71]. Calculations by Hendrickson[73] indicate that the barrier for conformational inversion in cyclopentane is 3-4 kcal/mole. If it is valid to draw analogies between cyclopentane and the furanose ring, this would indicate that at the temperatures studied, conformational interconversion would be fast on the n.m.r. time scale. It is quite likely therefore that the observed coupling constants are the result of an equilibrium between several conformations, not necessarily including the ^{0}V conformer chosen as most probable by the above method. This

would also account for the lack of a strong temperature dependence, as most conformations would be energetically accessible even at the lowest temperature studied.

The conformation chosen for uridine by a number of workers[4,67,76] places $C_{2'}$ or $C_{3'}$ or both out of the plane of the ring. Hruska et al.[4], and Prestegard and Chan[76] chose a C_2'-endo--C_3'-endo equilibrium, while Hall et al.[67] prefer the $V_2 \leftrightarrow {}^3T_2 \leftrightarrow {}^3V$ equilibrium. Either is quite reasonable, the primary consideration being to twist the 2',3' region so that the hydroxyl groups are no longer eclipsed. Since this situation is not present in aU it is not surprising that the conformation may be determined by other criteria, such as the CH_2OH - base ring steric crowding.

5. Conformation of the Exocyclic CH_2OH Group

It has been suggested[4] that the conformational rigidity of the phosphate backbone in polynucleotides may be due in part to rotational barriers about the five exocyclic bonds (C_4'-C_5', C_5'-O_5', O_5'-P, P-O_3', O_3'-C_3'). Sundaralingam[88], and Lakshminarayanan and Sasisekharan[89] have treated this problem, the former using x-ray data and models, the latter applying a theoretical treatment employing a simple hardsphere model for atoms. NMR has been applied to this problem to measure both the $H_5'P$ coupling constants[90] and the

$H_4'H_5'$ coupling constants[4,59].

The three classical staggered rotamers are shown in Figure 18. Assuming that the time spent in each conformation is long compared to the time spent rotating between them, then the 4'-5' coupling constants will be a weighted average of the couplings due to the three conformations. This is expressed by the equations below.

$$J_{4'5'_B} = P_I J_{IB} + P_{II} J_{IIB} + P_{III} J_{IIIB}$$

$$J_{4'5'_C} = P_I J_{IC} + P_{II} J_{IIC} + P_{III} J_{IIIC}$$

It has been suggested that oxygen-oxygen repulsions may alter the positions of the energy minima so that the classical staggered rotamers are no longer valid[59]. Allowing a limit of 15° for this repulsion between O_1' and C_5'-OH, calculations were performed for both the classical and repulsion-included cases. These calculations employ the Karplus relation, which is assumed to hold here, with two values of J^{180}. As a lower limit the values suggested by Abraham et al.[72] were chosen:

$$J^{\circ}=9.27\ H_z \text{ for } 0^{\circ} \leq \phi \leq 90^{\circ} \text{ and}$$

$$J^{180}=10.36 H_z \text{ for } 90^{\circ} \leq \phi \leq 180^{\circ}.$$

As an upper limit the values suggested by Lemieux (from reference 59) were taken:

Figure 18

Newman projections along the C_5'-C_4' bond showing the three staggered rotamers for aU.

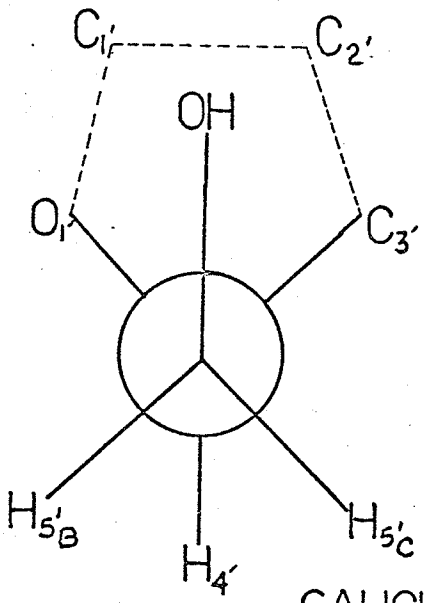

GAUCHE - GAUCHE

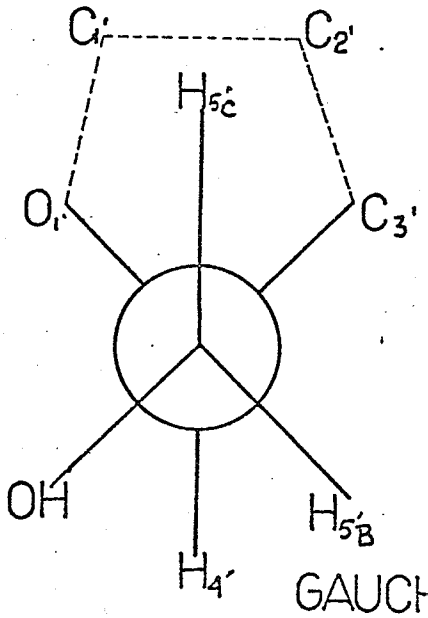

GAUCHE - TRANS

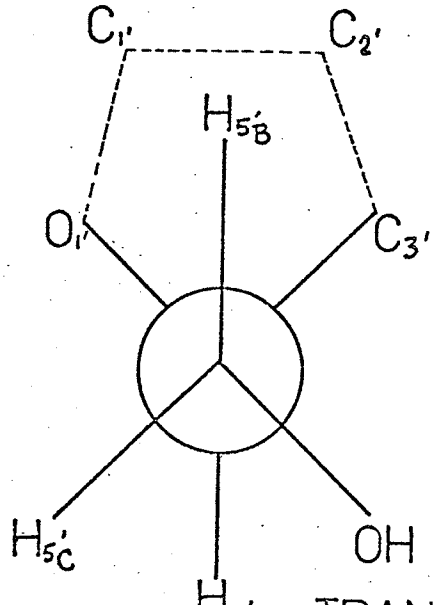

TRANS - GAUCHE

Table IV

ROTAMER POPULATIONS FOR aU

		Classical Staggered Rotamers				Rotamers with 1.5° O-O repulsion			
	J^{o}	9.27	9.27	9.27	9.27	9.27	9.27	9.27	9.27
	J^{180}	10.36	10.36	12.00	12.00	10.36	10.36	12.00	12.00
	$J_{4'5'B}$	3.1	5.5	3.1	5.5	3.1	5.5	3.1	5.5
	$J_{4'5'C}$	5.5	3.1	5.5	3.1	5.5	3.1	5.5	3.1
5°	PI	.45	.45	.54	.54	.37	.47	.51	.55
	PII	.43	.12	.35	.11	.35	.00	.25	.00
	PIII	.12	.43	.11	.35	.28	.53	.24	.45
	$J_{4'5'B}$	3.2	5.6	3.2	5.6	3.2	5.6	3.2	5.6
	$J_{4'5'C}$	5.6	3.2	5.6	3.2	5.6	3.2	5.6	3.2
30°	PI	.41	.41	.52	.52	.33	.44	.47	.54
	PII	.44	.15	.36	.12	.37	.02	.27	.00
	PIII	.15	.44	.12	.36	.30	.54	.26	.46
	$J_{4'5'B}$	3.4	5.5	3.4	5.5	3.4	5.5	3.4	5.5
	$J_{4'5'C}$	5.5	3.4	5.5	3.4	5.5	3.4	5.5	3.4
80°	PI	.40	.40	.50	.50	.31	.41	.46	.53
	PII	.43	.17	.36	.14	.37	.06	.27	.00
	PIII	.17	.43	.14	.36	.32	.53	.27	.45

$J^{o}=9.27\ H_z$ for $0^{o} \leq \phi \leq 90^{o}$ and

$J^{180}=12.00\ H_z$ for $90^{o} \leq \phi \leq 180^{o}$.

The notation in Figure 18, as $H_{5'B}$ and $H_{5'C}$, was intentionally used to avoid confusion with the $H_{5'A}$ and $H_{5'B}$ assigned by spectral position. It was not feasible to identify $H_{5'A}$ or $H_{5'B}$ with a specific hydrogen atom.

Comparing the data for aU, as presented in Table IV, with that for uridine[59], it appears that the gauche-gauche rotamer is less favoured in aU than in uridine. This may be due to a repulsion between the 5'-O and the 2'-O. While taking care not to ascribe too much importance to the numbers presented, it also appears that the population of rotamer I, the gauche-gauche form, decreases slightly with increasing temperature.

6. Evidence for the presence of several long-range couplings.

Table II lists values for three long-range couplings in the furanose ring: $J_{1'3'}$, $J_{3'5'A}$, and $J_{3'5'B}$. The first of these could be checked by double resonance experiments, and its existance was verified, although the broadness of the respective peaks prevented determination of the sign. The last two couplings, $J_{3'5'A}$ and $J_{3'5'B}$, were not observed experimentally, however it was impossible to achieve a close fit to the 5'

region in the calculated spectra without introducing these parameters. The tight coupling of the 3', 4', and 5' regions gives rise to a multitude of transitions and correspondingly wide peaks, making double irradiation experiments on $J_{3'5'_A}$ and $J_{3'5'_B}$ inconclusive. If such a coupling does exist, it would appear to be a "through-space" effect, a consequence of the proximity of the 3'-H and the 5'-H's. The predominance of the gauche-gauche rotamer in U and cU would increase the average separation of the 3'-H and the 5'-H's, accounting for the absence of any 3'-5' coupling in these compounds.

A similar "through-space" coupling has been observed by Goldstein[74] for a methoxy group on benzene, and by Wasylishen[75] for several molecules, two of which are shown in Figure 19.

As the size and sign of this coupling are still in doubt, it will not be discussed further, only noting its possible existance.

The splitting of 0.2 H_z which is seen in the H-2' peaks at 80°C was initially thought to be due to another long-range coupling, probably to H-4'. On the basis of repeated calculations however, it was decided that this splitting is probably due to virtual coupling to H_4'. The best computer fit achieved to the rest of the spectrum produced a 0.1 H_z splitting in the H-2' peaks, and

Figure 19

Two molecules which show evidence of a "through-space" coupling, the magnitude of which is shown for each[75].

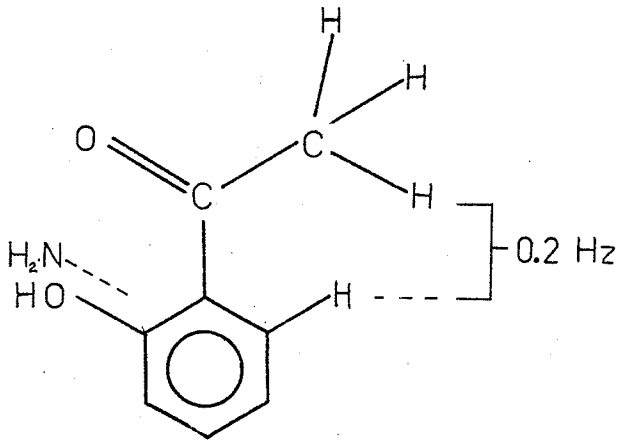
H
H
O
C
C
H
0.2 Hz
H₂N
HO
H

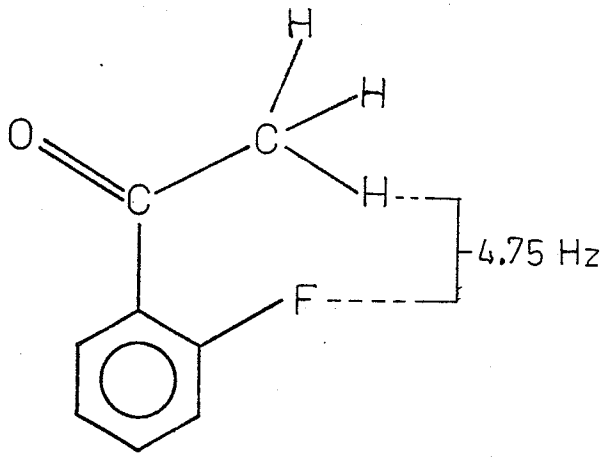
H
H
O
C
C
H
4.75 Hz
F

introduction of various long-range couplings failed to improve the fit, in most cases making it worse. More evidence will be required before any definite conclusions can be drawn.

B. 2,2' - anhydrouridine

1. Spectral Assignment

The observed spectra of anhydrouridine at 5°C, 30°C, and 80°C are shown in Figures 20-22 accompanied by the computer-simulated spectra. Table V lists the values of the chemical shifts and coupling constants for cU and aU (in parentheses) at all three temperatures, and for uridine at 28°C.

The most striking feature of these spectra, especially at 80°C, is the increase in the number of lines resolved. It was noted for aU that the observed couplings may be time-averages, and that the sugar ring is altering its geometry rapidly. It is shown below that the fine structure in the spectrum of cU is due to long-range couplings between the sugar protons. Such couplings are usually highly stereospecific and it is likely that in aU they are washed out by the rapidly changing structure, while the anhydro linkage in cU gives the system a much greater rigidity, allowing free movement only in the C_4' and C_5' region.

The intial spectral assignment was made by comparison with uridine and arabinouridine. Slight variations in the shifts occur with temperature, but these are not large enough to alter the appearance of the spectrum significantly. With this in mind, the assignments are discussed for the 80°C spectrum, the other two

Figure 20

The 100 MHz spectrum of anhydrouridine at 5°C with the scale in PPM to low field of DSS. The lower spectrum is the experimental one, while the upper is a computer-fitted simulation.

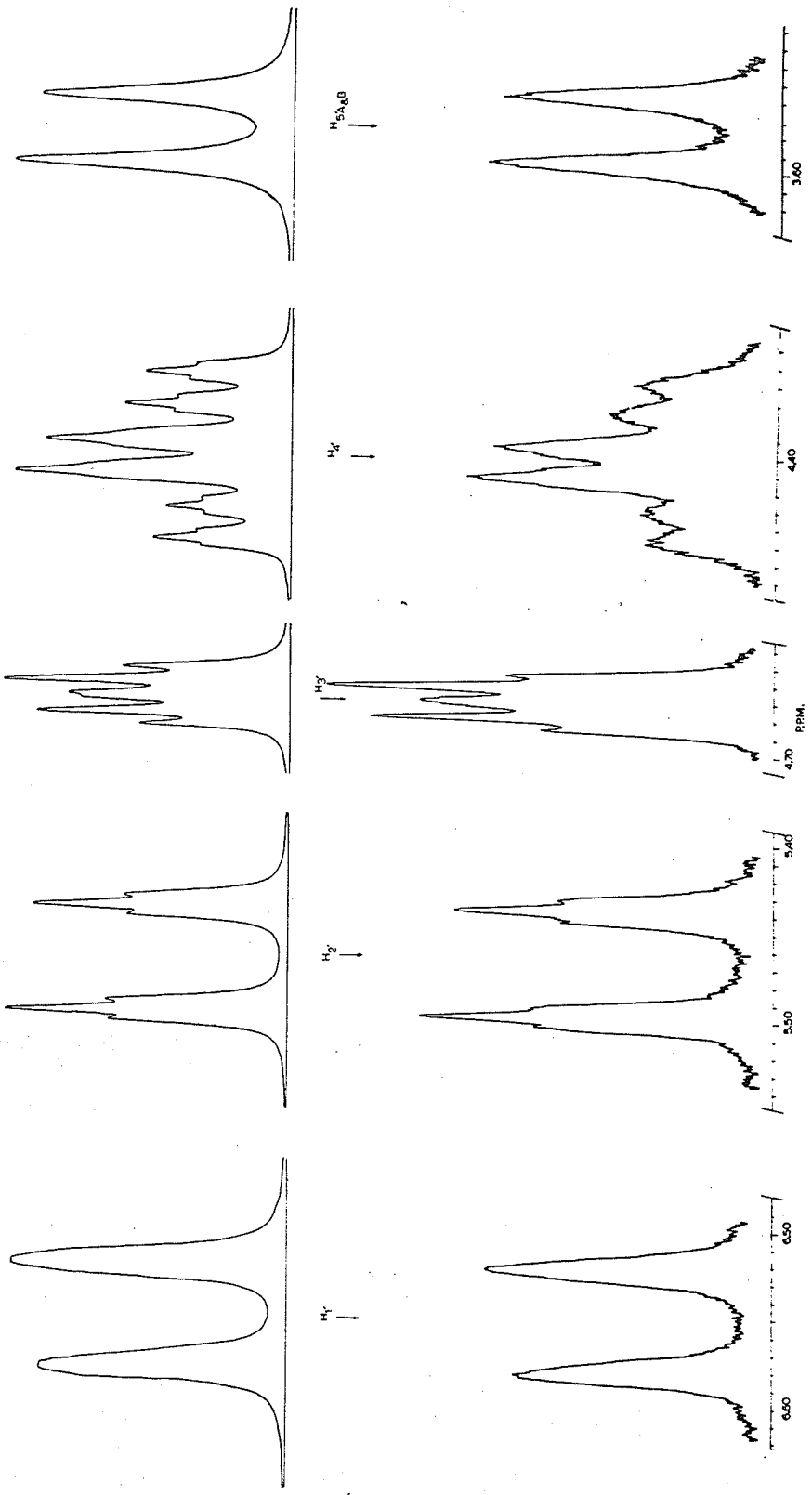
H5A&B
H4'
H3'
H2'
H1'
6.50
5.50
5.40
4.70
4.40
3.60
P.P.M.

Figure 21

The 100 MHz spectrum of anhydrouridine at 30°C with the scale in PPM to low field of DSS. The lower spectrum is the experimental one, while the upper is a computer-fitted simulation.

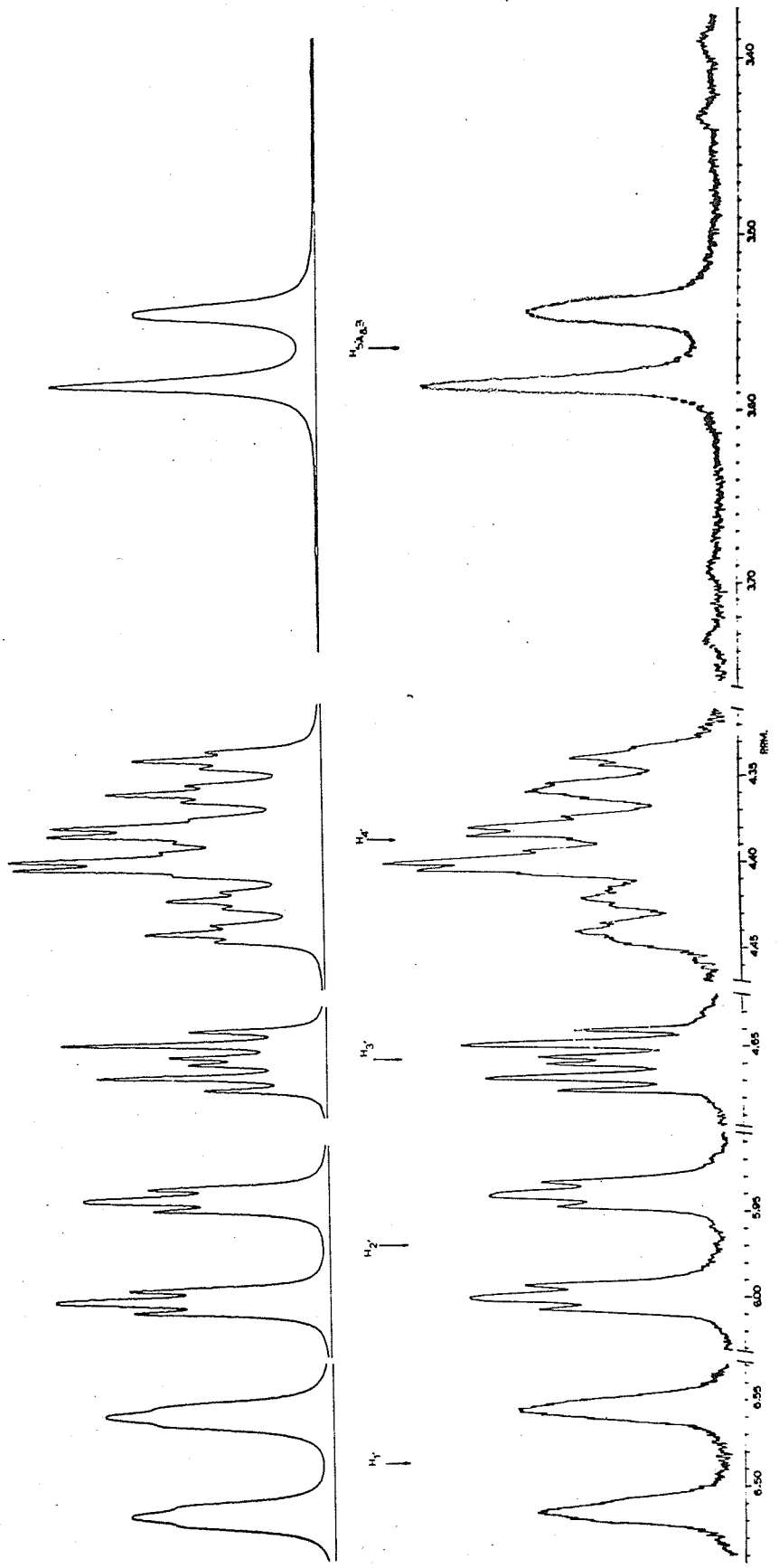
H1'
H2'
H3'
H4'
H5A,B,3'
6.50
6.55
6.00
5.95
4.65
4.45
4.40
4.35
3.70
3.60
3.50
3.40
PPM.

Figure 22

The 100 MHz spectrum of anhydrouridine at 80°C with the scale in PPM to low field of DSS. The lower spectrum is the experimental one, while the upper is a computer-fitted simulation.

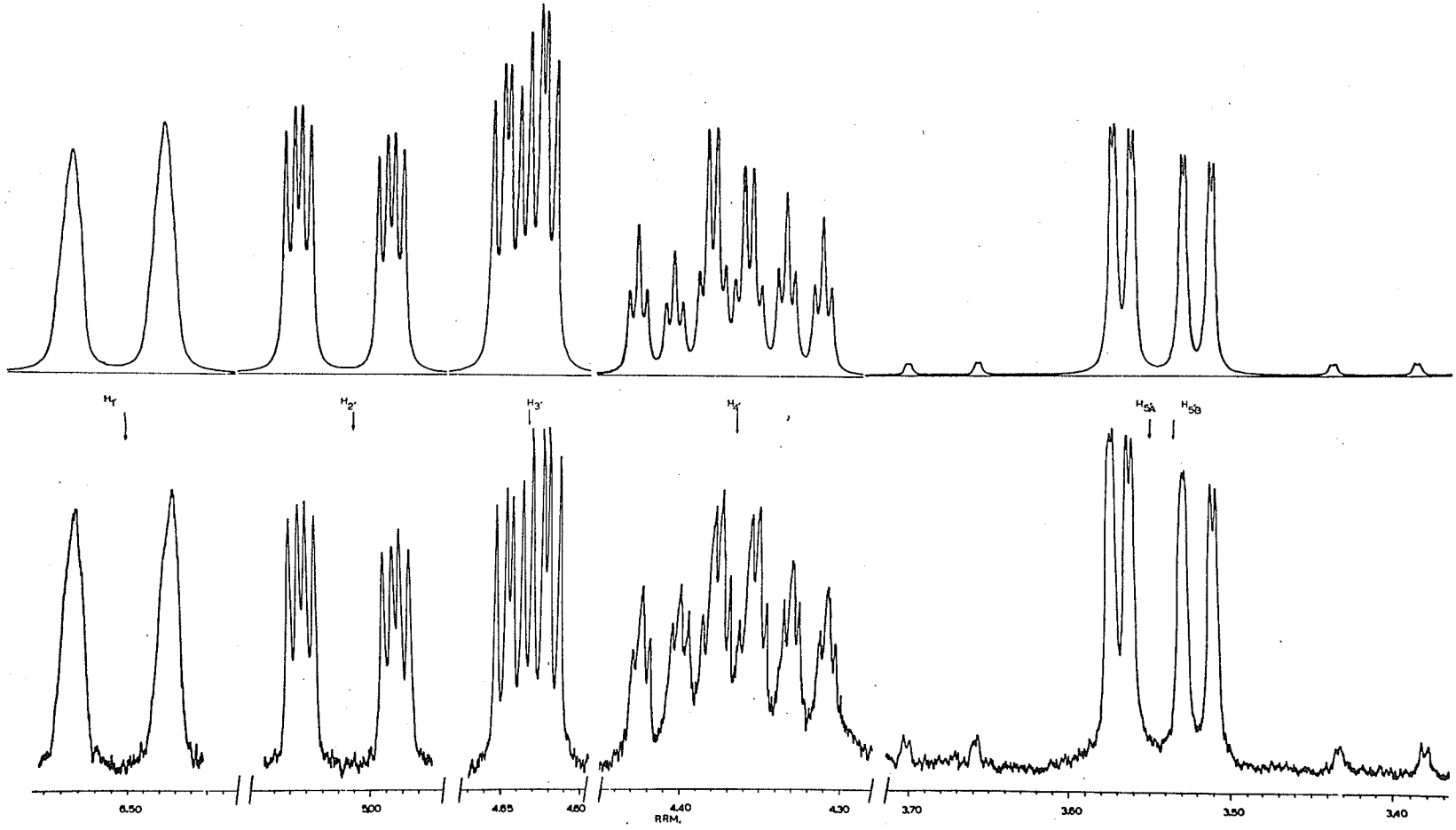
H1'
H2'
H3'
H4'
H5A
H5B
6.50
5.00
4.65
4.60
4.40
4.30
3.70
3.60
3.50
3.40
PPM.

Table V

Shifts (PPM downfield from TMS) & Coupling Constants (Hz)
for aU and cU (in parentheses)

	Uridine 28°	5°		30°		80°	
H_6	7.862	7.934	(7.865)	7.917	(7.839)	7.881	(7.802)
H_5	5.887	6.184	(5.851)	6.192	(5.860)	6.189	(5.857)
H_1'	5.901	6.549	(6.175)	6.534	(6.169)	6.502	(6.147)
H_2'	4.341	5.472	(4.400)	5.470	(4.398)	5.465	(4.396)
H_3'	4.222	4.668	(4.124)	4.657	(4.128)	4.632	(4.133)
H_4'	4.128	4.401	(3.983)	4.390	(3.988)	4.365	(3.987)
$H_{5'A}$	3.907	3.577	(3.911)	3.576	(3.907)	3.577	(3.902)
$H_{5'B}$	3.803	3.576	(3.828)	3.553	(3.827)	3.515	(3.829)
$J_{1'2'}$	4.4	5.95	(5.00)	5.9	(5.11)	5.8	(5.10)
$J_{1'3'}$	-	-0.81	(0.30)	-0.75	(0.30)	-0.64	(0.30)
$J_{1'4'}$	-	-0.42	-	-0.46	-	-0.52	-
$J_{1'5'A}$	-	-	-	-	-	0.252	-
$J_{1'5'B}$	-	-	-	-	-	0.314	-
$J_{2'3'}$	5.3	0.7	(4.72)	0.8	(4.53)	1.0	(4.33)
$J_{2'4'}$	-	0.535	-	0.54	-	0.55	-
$J_{3'4'}$	5.5	1.8	(5.71)	1.9	(5.53)	2.3	(5.44)
$J_{4'5'A}$	3.0	2.9	(3.05)	3.3	(3.23)	4.2	(3.41)
$J_{4'5'B}$	4.4	4.7	(5.47)	4.9	(5.55)	5.1	(5.51)
$J_{5'A5'B}$	-12.7	-13.89	(-12.64)	-13.5	(-12.49)	-12.6	(-12.40)
J_{56}	8.0	7.4	(8.15)	7.4	(8.10)	7.4	(8.15)

temperatures being very similar.

The doublet at 7.881 ppm was assigned to H_6 of the uracil base since it is adjacent to a nitrogen atom, as in U and aU. The doublet at 6.189 ppm shares the same splitting, and was consequently assigned to H_5 of the uracil moiety. The small couplings to H_1' that were observed in aU are no longer observed. This is discussed in section 2.

The region around 4.365, 3.577, and 3.515 ppm shows the characteristic ABC pattern which was attributed to H_4' and the two H_5' protons of the furanose in aU and U. For cU, the 4.365 ppm value corresponds to H_4', 3.577 ppm to $H_5'_A$, and 3.515 ppm to $H_5'_B$.

The H_1' resonance is adjacent to a nitrogen atom, appearing as a result near H_6 at 6.502 ppm. This doublet consists of two very broad peaks, separated by ~6 H_z. It is shown later that the broadness is due to the presence of a number of long-range couplings, to H_3',H_4', and both H_5' protons. It may never be possible to resolve this fine structure as the resonance may be further broadened by the nearby N_1 nitrogen atom.

The resonances at 5.465 ppm, and 4.632 ppm were assigned to H_2' and H_3' respectively by comparison of the large vicinal couplings. The assignments were verified by double resonance experiments.

The computer-simulated spectrum for 80°C is an excellent fit, including the small long-range couplings mentioned above. The calculated spectrum for 30°C is still quite good, but at 5°C the increasing broadness of the peaks makes it almost impossible to assign specific line positions to the individual transitions. The values used for the calculated spectrum at 5°C are straight-line extrapolations of the shifts vs temperature for 30°C and 80°C. They provide the basis for an acceptable simulation of the observed spectrum.

In a C^{13} magnetic resonance study of a number of pyrimidine nucleosides, Jones et al.[40] note that an amino or methoxy substituent at C_2 produces a downfield shift of the base protons similar to that occuring on formation of the anhydro linkage, and conclude that the C^{13} shifts of cU can be explained in terms of substituent effects. Their data show a downfield shift for C_5 and an upfield shift for C_6 compared to those for uridine. In an earlier paper[39] they showed a close correlation between C^{13} shifts and π-electron densities. Thus the upfield shift of C_6 would correspond to an increase in π-electron density and the downfield shift of C_5 would mean a decrease. However, the pmr data in Table V show a downfield shift for both H_6 and H_5 with respect to uridine.

While Jones et al.[40] suggest that the C^{13} shifts are due to substituent effects and that there is little interaction between the sugar and pyrimidine moieties, it seems likely that H_6 projecting some distance over the sugar ring in uridine, may be shielded by it. The downfield shift of H_6 in cU may thus be due to the loss of this furanose shielding as formation of the anhydro linkage turns the base so H_6 is no longer over the ring (see Figure 23).

Comparison of the shifts of the sugar protons of cU with those of aU, shows a downfield shift for H_1', H_2', H_3', and H_4' (Table V). The change in sugar structure makes this comparison more appropriate than one between cU and U. The deshielding, which is twice as great for H_2' as for H_1' and H_3' can be described in terms of an electron-withdrawing effect through the anhydro bridge. The ability of the carboxyl group to withdraw electrons through an oxygen is shown in the model compounds I and II.

I $CH_3-\overset{*}{C}H_2-O-CH_2-CH_3$ $\quad \nu_{H*}= 3.36$ ppm

II $CH_3-\overset{*}{C}H_2-O-C(=O)-Me$ $\quad \nu_{H*}= 4.06$ ppm

III

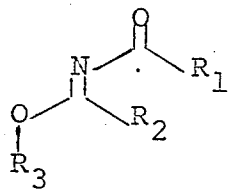

Figure 23

aU and cU viewed along the N_1 to C_1' direction showing the relative positions of the plane of the base ring.

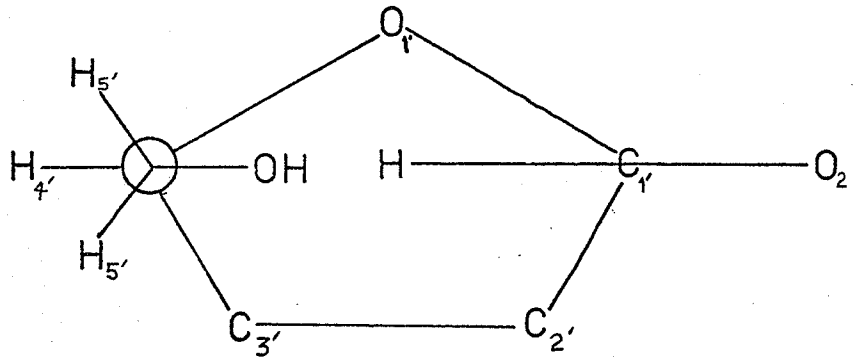

aU

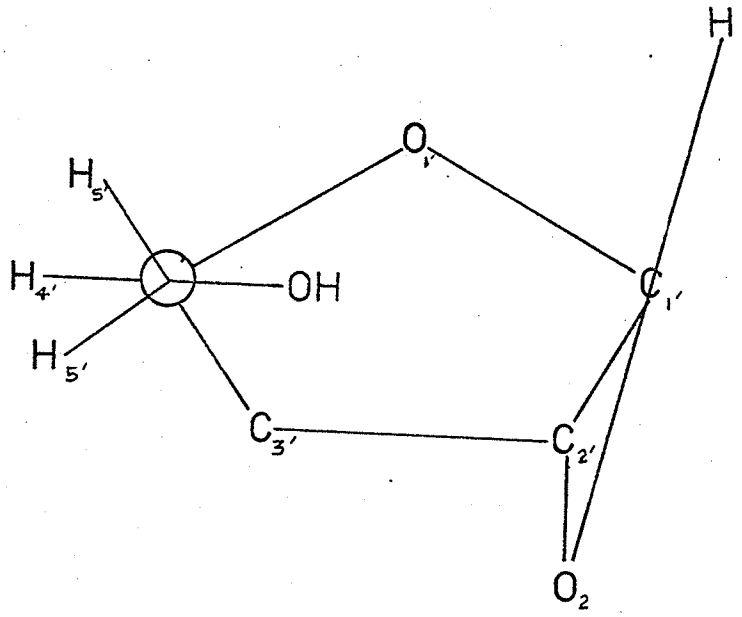

cU

Compound III shows the segment of cU being considered. The double bond between C_2 and N_3 makes this a vinylogous ester, so the analogy to II is reasonable. Moreover the pyrimidine moiety has the ability to stabilize a negative charge through delocalization, as shown in Figure 24. This idea was first suggested by Doerr et al. for an imino-bridged analog[102]. C^{13} magnetic resonance studies by Jones et al.[40] show a substantial downfield shift for the C_2' nucleus of cU compared to U and aU. This would indicate a lower electron density at C_2' in cU which would agree with the proposed delocalization into the base ring. The differences in the shifts of the other sugar and base carbons are smaller and somewhat ambiguous. Since C^{13} shifts vary with bond order as well as total charge[40] it seems unwise to attempt any further rationalization of these C^{13} data until calculated charge densities are available.

It is worth noting that the C^{13} shifts for the 5'-anhydro analog show the same downfield shift at C_5'. This means ring strain is unlikely to be the cause of the downfield shift in cU.

The fact that the deshielding is much greater at H_2' than at H_1' or H_3' is to be expected, as inductive effects drop off rapidly with distance. However, H-4' shows a rather larger deshielding than one would expect by this inductive argument considering it is one bond

Table VI

Relative shifts of the sugar protons in U, aU, cU at 30°C

	cU - U (ppm)	cU - aU (ppm)
H_1'	0.633	0.366
H_2'	1.129	1.072
H_3'	0.435	0.528
H_4'	0.262	0.402
$H_5'_A$	-0.331	-0.331
$H_5'_B$	-0.250	-0.275

Figure 24

cU showing the possible pattern of charge delocalization into the ring.

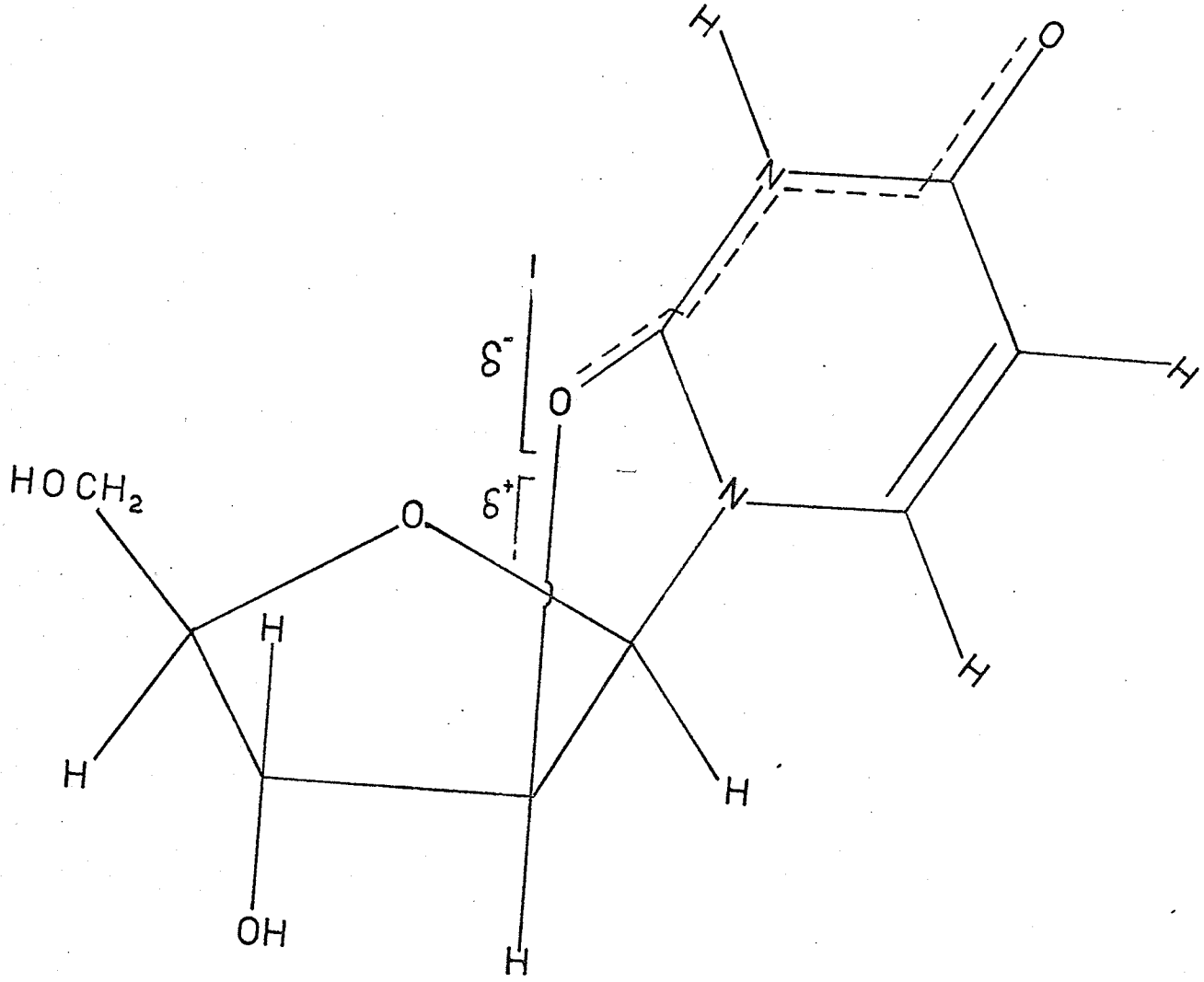
H
O
N
δ⁻
O
H
HOCH₂
O
δ⁺
N
H
H
H
H
OH
H

further from O_2 than either H_1' or H_3'. As noted in the section on aU, H_4' shifts are often somewhat anomalous, and no further attempt to account for this value will be attempted here, except to note that the C^{13} data[40] does indicate a large deshielding at C_4', also unexplained.

The $H_5'_A$ and $H_5'_B$ protons show a large upfield shift, 0.23 ppm and 0.275 ppm respectively, when compared to aU at 30°C. This cannot be accounted for by any of the mechanisms previously discussed. It is unlikely to be an effect of the change in rotamer populations, as none was noticed in aU. The only other significant change is the rotation of the base ring through 90° to form the anhydro linkage, bringing O_2 nearer to the C_5' protons and allowing the possibility of shielding by the oxygen.

2. Anomeric Configuration and Sugar-Base Torsion Angle

Examination of the H_1' shifts in order to determine anomeric configuration is much less informative than for aU, the results being somewhat ambiguous. However, the compound was prepared by D.Iwacha of this department using a procedure known to result in the β-anomer exclusively.

The sugar-base torsion angle is fixed by the C_2'-O-C_2 anhydro linkage at approximately 110° to the

anti conformation observed for U and aU. This would explain why no long-range couplings from H_1' to H_5 or H_6 are observed. H_1' is now almost perpendicular to the base ring - a highly unfavourable orientation for long-range coupling.

3. Conformation of the Furanose Ring

Determination of the conformation of the furanose ring was approached in the same manner as for aU. The fused triple-ring system was expected to limit changes in conformation to the $C_3'-C_4'-O_1$ region, and x-ray crystallographic studies[101] indicate that the V_3 conformation is favoured. Application of the Karplus relation to $J_{1'2'}$, $J_{2'3'}$, and $J_{3'4'}$ with $J^{o}=9.27$, $J^{180}=10.36$, gave values for the dihedral angles as shown in Table VII.

Strict application of the method of Hall et al.[67] to the range of conformations given in Table VII is not completely satisfactory, the prediction being that the V_1 conformer is favoured. In this form, $\phi_{3'4'}$ should be 120^{o}, which is very close to that value calculated from $J_{3'4'}$. However for V_1, $\phi_{1'2'}$ is 50^{o}, and $\phi_{2'3'}$ is 90^{o}. The calculated values, from the observed J's, are 35^{o} and 109^{o} respectively. Moreover, an examination of Dreiding models indicates that the fused rings make the V_1 conformation, as originally defined

Table VII

a) Calculated Dihedral Angles for the cU Furanose Ring

$J^{\circ} = 9.27$

$J^{180} = 10.36$

Temp.($^{\circ}$C)	$J_{1'2'}$	$\phi_{1'2'}$	$J_{2'3'}$	$\phi_{2'3'}$	$J_{3'4'}$	$\phi_{3'4'}$
5°	5.95	34.9	0.7	107.9	1.8	116.6
30°	5.9	35.3	0.8	108.8	1.9	117.3
80°	5.8	35.9	1.0	110.6	2.3	119.9

continued...

Table VII - continued

b) Dihedral Angles for the Conformations of CYCLOPS

Conformation	$\phi_{1'2'}$	$\phi_{2'3'}$	$\phi_{3'4'}$
^{o}V	30	120	150 X
$^{o}T_{1}$	50	90	150 X
V_{1}	50	90	120
$^{2}T_{1}$	60	70 X	100
^{2}V	50	70 X	90
$^{2}T_{3}$	50	60 X	90
V_{3}	30	70	70 X
$^{4}T_{3}$	20	70	60 X
^{4}V	0	150	70 X
$^{4}T_{o}$	20	100	50 X
V_{o}	30	120	90 X
$^{1}T_{o}$	50	140 X	100
^{1}V	50	150 X	120
$^{1}T_{2}$	60	170 X	140
V_{2}	50	170 X	150
$^{3}T_{2}$	50	180 X	170
^{3}V	30	170 X	170
$^{3}T_{4}$	20	170 X	180
V_{4}	0	150 X	170
$^{o}T_{4}$	20	140 X	170

X - indicates parameter with greatest deviation from the experimental values.

by Hall, extremely strained. If the assumption of maximal puckering is relaxed somewhat, allowing C-1' to approach the plane of the other four atoms, then the dihedral angles approach the calculated values quite closely. According to the calculations by Abraham and McLauchlan[68], the "maximal puckering" described by Hall et al.[67] requires that the out-of-plane atom be bent down approximately 50° from the plane of the other four. The "modified V_1" conformation suggested here requires a bend of 35° down, and predicts the values of $\phi_{1'2'}$, $\phi_{2'3'}$, and $\phi_{3'4'}$ to be 35°, 100°, and 120° respectively.

The Karplus relation is sensitive to the presence of electronegative substituents, and while the values of J^{o} and J^{180} were chosen for carbohydrate systems, the delocalized structure proposed in section B-1 acts to withdraw electrons from $C_{2'}$. This should reduce the observed value of $J_{1'2'}$ and $J_{2'3'}$, and increase $J_{3'4'}$, making $\phi_{1'2'}$ and $\phi_{3'4'}$ too large, and $\phi_{2'3'}$ too small. V_1 still appears to be the best fit however, and the V_3 conformation proposed by Brown et al.[101] from x-ray crystallographic studies of the 5'-deoxy-5'-iodo-O^2, 2'-cyclouridine provides a very poor fit, even allowing for errors in the calculated values of ϕ due to this electron-withdrawing effect.

4. Conformation of the exocyclic CH_2OH group

Following the same analysis as in section A5, the proportions of each of the possible rotamers was calculated for both the classical staggered forms and the 15° oxygen-oxygen repulsion forms at all three temperatures. These values are presented in Table VIII.

As in aU, the pattern is quite complex. At 5°C the gauche-gauche rotamer (I) is shown to be clearly preferred, by both the classical calculations and those allowing for O-O repulsion. At 30°C the preference still exists, but to a lesser degree. While the population of rotamer I drops below 0.5 in the cases where J^{o}=9.27, J^{180}=10.36, no other single rotamer is more favoured. At 80° this is no longer true, the prefered rotamer depending upon the proton assignment, the J^{o} values, and the choice of classical or 15°-repulsion structures. The general trend however is again toward a decrease in the population of the gauche-gauche rotamer with increasing temperature.

In uridine, the C-5' hydroxyl comes very near the H-6 of the uracil base in the gauche-gauche rotamer, It has been suggested[59], that this may account for the differing responses of H-5 and H-6 to changes in temperature. While the change in conformation about the N-glycosyl bond means that the interactions between the C-5' OH and H-6 in cU are likely to be less than in

Table VIII

ROTAMER POPULATIONS FOR cU

	Classical Staggered Rotamers				Rotamers with 15° O-O repulsion			
J_o	9.27	9.27	9.27	9.27	9.27	9.27	9.27	9.27
J_{180}	10.36	10.36	12.00	12.00	10.36	10.36	12.00	12.00
$J_{4'5'B}$	2.9	4.7	2.9	4.7	2.9	4.7	2.9	4.7
$J_{4'5'C}$	4.7	2.9	4.7	2.9	4.7	2.9	4.7	2.9
5° PI	.56	.56	.64	.64	.54	.62	.64	.70
PII	.33	.11	.27	.09	.20	.00	.13	.00
PIII	.11	.33	.09	.27	.26	.38	.23	.30
$J_{4'5'B}$	3.3	4.9	3.3	4.9	3.3	4.9	3.3	4.9
$J_{4'5'C}$	4.9	3.3	4.9	3.3	4.9	3.3	4.9	3.3
30° PI	.49	.49	.56	.56	.45	.53	.57	.61
PII	.35	.16	.31	.13	.25	.00	.17	.00
PIII	.16	.35	.13	.31	.30	.47	.26	.39
$J_{4'5'B}$	4.2	5.1	4.2	5.1	4.2	5.1	4.2	5.1
$J_{4'5'C}$	5.1	4.2	5.1	4.2	5.1	4.2	5.1	4.2
80° PI	.35	.35	.46	.46	.28	.30	.43	.46
PII	.38	.27	.32	.22	.32	.21	.23	.12
PIII	.27	.38	.22	.32	.40	.49	.34	.42

uridine, the above explanation may account for the fact that here too, the H-6 shift shows a greater temperature dependence than the H-5 shift.

5. Evidence for a number of Long-Range Couplings

A number of papers have noted couplings between H-1' and the protons of the base rings. Reported below is evidence for several four- and five-bond couplings within the sugar moiety.

Among the coupling constants listed in Table V are values for $J_{1'3'}$, $J_{1'4'}$, $J_{2'4'}$, and at 80°C only, $J_{1'5'A}$, $J_{1'5'B}$. The splittings due to these couplings are clearly distinguishable at 80°C, at which temperature they were first detected. They were all verified by double resonance techniques, and provide a much improved fit when introduced into the computer-simulated spectrum. At 30°, only $J_{1'3'}$, $J_{1'4'}$, and $J_{2'4'}$ are still distinct, and it is possible to simulate the spectrum without introducing any 1'-5' couplings. While these 1'-5' couplings may still be present, there was no way to estimate their size, due to the broadness of the observed peaks, consequently it was decided not to assign a value to them. Also, since the values for 5°C were taken by extrapolation of the 80°C and 30°C values, $J_{1'5'A}$ and $J_{1'5'B}$ do not appear here either.

The apparent splittings in the $5'_A$ and $5'_B$ regions of the spectrum are somewhat less than the actual couplings involved. The values reported are those produced by the iterative form of LAOCNN3 used to fit the calculated spectrum to that observed. This experimental narrowing has been calculated by Jackman and Sternhell[44] for perfect Lorenzian line shapes. The correction factor calculated by them is shown by the graph in Figure 25.

The signs of $J_{1'3'}$, $J_{1'4'}$ and $J_{2'4'}$ were verified by double resonance experiments. Those for $J_{1'5'_A}$ and $J_{1'5'_B}$ were produced by the iterative form of LAOCN 3.

It is difficult to account for the signs of $J_{1'3'}$, $J_{1'4'}$, and $J_{2'4'}$ by any of the present theoretical treatments. Barfield[55,100] has calculated values for substituted and unsubstituted propanic fragments which agree well with a number of experimental values. Table IX lists his values for $^4J_{HH'}$ in propane calculated by the INDO (Intermediate Neglect of Differential Overlap) technique. If the furanose ring in cU were planar, the coupling paths would resemble propanic fragments for which Barfield calculates the following values (from Table IX):

$J_{1'3'}(120^\circ,240^\circ)= -0.29$ Hz, $J_{1'4'}(120^\circ,120^\circ)= -0.12$ Hz, and $J_{2'4'}(120^\circ,120^\circ)= -0.12$ Hz, for the unsubstituted fragments. Ring puckering in the V_1 conformation would

Figure 25

The effect of imperfect resolution on the apparent magnitude of splitting of resonances. (Ref.44,p.313)

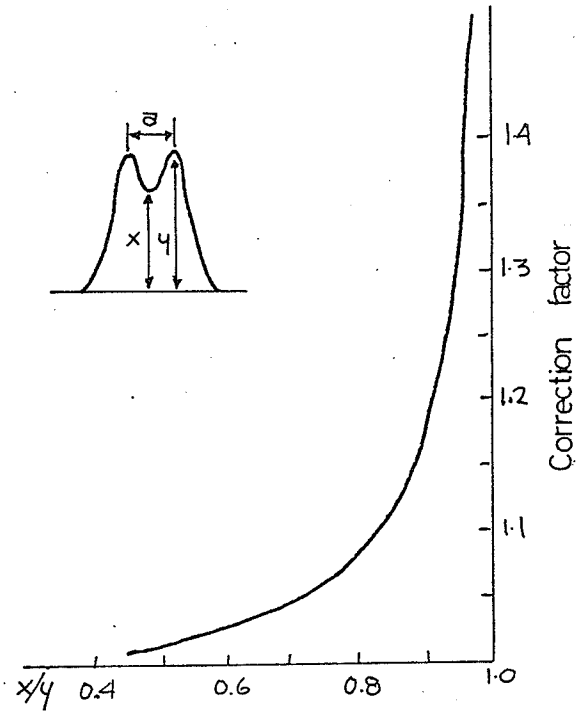
a
x
y
1.4
1.3
1.2
1.1
1.0
Correction factor
x/y
0.4
0.6
0.8

alter the dihedral angles Ø and Ø' (defined in Table IX) in such a manner as to make $J_{1'3'}$ and $J_{1'4'}$ more negative and $J_{2'4'}$ more positive.

Extending the calculations to substituted propanic fragments, Barfield[55] proposes that the effect of an inductive or hyperconjugative substituent at any of the three carbons should produce a positive shift in the values of $^4J_{HH'}$ relative to the propane values except for a hyperconjugative substituent at C-3 which should produce a negative shift in the value of $^4J_{HH'}$. The inductive electron withdrawal at $C_{2'}$ through the anhydro linkage should have a considerable effect on the values of $J_{1'3'}$ and $J_{2'4'}$. The size of the effect is strongly conformation-dependent[55], which may explain in part why $J_{2'4'}$ seems to be affected more than $J_{1'3'}$. There are undoubtedly other factors which a semi-empirical treatment like INDO neglects, but it is encouraging to see that it agrees qualitatively with the observed values for these long-range couplings in cU.

No calculations have appeared on the effect of inserting a heteroatom in place of C-2 of the propanic fragment. In the example shown below, the signs of $J_{2,5}$ <u>trans</u> and $J_{2,5}$ <u>cis</u> are both positive[105,106], while the $J_{1'4'}$ observed in cU is more negative than that predicted by Barfield's calculations. The example is slightly different however, in that it possesses a

double bond between C-3 and C-4. It seems possible that the heteroatom and the double bond have opposing influences on the sign of a ^{4}J in these cases.

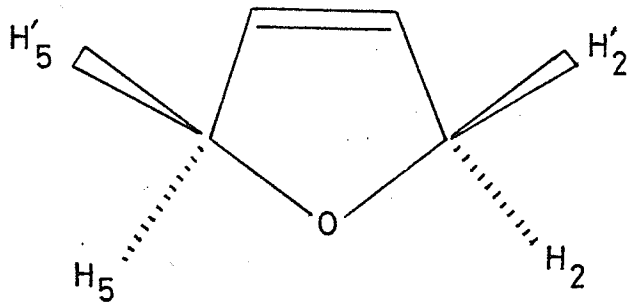

Chapter VI

Summary and Conclusions

Analyses of the proton magnetic resonance spectra of arabinouridine and anhydrouridine have been carried out for 5°C, 30°C, and 80°C. Interpretation of the shifts and coupling constants for these six spectra provide the basis for a complete structural analysis of each molecule.

The β-anomer of arabinouridine is shown to exist in the anti conformation about the glycosidic bond with less rotational freedom than in uridine due to the presence of the 2'-hydroxyl group. Coupling constants for the furanose protons indicate that the O-endo (^{O}V) conformation is favoured, but the energy barrier to ring flexing is so low that most other conformations are probably accessible at the temperatures studied. Uridine has been shown to favour the gauche-gauche rotamer about the exocyclic bond and the same is found to be true for aU, although the preference is less pronounced and decreases with increasing temperature. A number of long-range couplings are observed, one of which ($^{5}J_{1'5}$) supports the suggestion that the base ring is in the anti position and has little freedom of movement. The other long-range couplings, between furanose protons, are interesting in that they have not been previously reported. However, they are not readily interpreted in terms of particular structural characteristics. They will become more useful

when similar values are obtained for other nucleosides to which comparisons can be made.

Anhydrouridine was also studied as the β -anomer, and the absence of any long-range couplings from H_1' into the base protons confirmed the expectation that the anhydro linkage holds the base at right angles to the orientation observed in aU and U. The furanose ring is apparently in the H_1'-exo (V_1) conformation, despite previous reports that the V_3 conformation is favoured in the crystal form. Rotamer preferences are less pronounced than in either U or aU. Although the gauche-gauche form is slightly predominant at lower temperatures, this decreases with increasing temperature until at 80°C, no rotamer is clearly favoured. Long-range couplings are even more in evidence than in aU. The altered sugar-base torsion angle means that $^5J_{1'5}$ and $^4J_{1'6}$ are no longer observed, but the anhydro linkage apparently makes the furanose ring sufficiently rigid that several new coupling paths become favourable. While the long-range couplings do serve in some cases as additional support for the structures proposed, there are no simple relations by which they can be related to definite structural features.

Chapter VII

Suggestions for Future Research

One of the biggest problems in nuclear magnetic resonance studies of nucleosides is the use of dilute, aqueous solutions. These have always been chosen so that the results would have direct application to biological systems. Dilute solutions in any solvent are less satisfactory because of the poor signal-to-noise ratio, but aqueous (D_2O) solutions may be presenting an additional complication by causing broading of the lines. While other solvents such as DMSO may cause shift changes that affect the biological significance of the results, coupling constants should remain much the same. A comparitive study of solvents at various concentrations could suggest a number of alternative solutions for which the differences from aqueous nucleoside solutions were known. These could then be used in conjunction with aqueous studies to provide information on the fine structure due to long-range coupling interactions.

Further examination of the relationship between vicinal couplings and furanose conformation is required in order to choose the correct conformation with some degree of certainty. The range of dihedral angles chosen by various authors for any one conformation, and the uncertainty about the values of J^{o} and J^{180} to be used in the Karplus relation make the choice of any particular conformation somewhat difficult. Perhaps

with the low energy barrier to ring flexing the concept of a favoured conformation should be restricted to cases such as the ribose sugars where steric crowding makes some conformations highly unfavourable.

Several excellent C^{13} magnetic resonance studies on nucleosides have appeared and the information provided serves to complement that obtained by proton magnetic resonance. An extension of C^{13} and H^{1} magnetic resonance to nucleotides, plus the inclusion of P^{31} magnetic resonance, would provide a basis for intensive studies of the dimers and possibly the polymers. The analysis of the combined data may be able to provide a complete structural analysis of these more complex systems.

One of the problems noted by Barfield[55] in his discussion of long-range couplings was the absence of a systematic study of small long-range couplings in substituted propanes. Such data could provide a basis for a more precise evaluation of the substituent and conformational dependence of $^{4}J_{HH}$, which in turn could be applied to the long-range furanose couplings. Information gained in this manner would serve as corroboration for the furanose conformations established by use of vicinal couplings.

Bibliography

1. Grey,A.A., Smith,I.C.P., and Hruska,F.E., J.Am. Chem.Soc. 93, 1765 (1971).

2. Rohrer,D.C., and Sunderalingham,M., J.Am.Chem.Soc. 92, 4950 (1970).

3. Dugaiczyk,A., Biochemistry 9, 1557 (1970).

4. Hruska,F.E., Grey,A.A., and Smith,I.C.P., J.Am. Chem.Soc. 92, 4088 (1970).

5. Philips,G.R., Nature 223, 374 (1969).

6. Holley,R.W., Apgar,J., Everett,G.A., Madison,J.T., Marquisse,W., Merill,S.H., Penswick,J.R., and Zamir,A., Science 147, 1462 (1965).

7. Cold Spring Harbour Symp. Quant. Biol. 31 (1966).

8. Mahler,H.R., and Cordes,E.H., Biological Chemistry, Harper and Row, New York, 1966, p.130.

9. Momparler,R.L., Biochem.Biophys.Res.Comm. 34,465 (1969).

10. Nagyvary,J., Provenzale,R., and Clark,Jr.,J.M., ibid 31, 508 (1968).

11. Suhadolnik,R.J., Nucleoside Antibiotics, Wiley-Interscience, New York, 1970, p.151.

12. Maurizot,J.C., Wechter,W.J., Brahms,J., and Sadron,C., Nature 219, 377 (1968).

13. Ts'o, P.O.P., Schweizer,M.P., and Hollis,D.P. Ann.New York Acad.of Sci. 158,256 (1969).

14. Guschlbauer,W., and Privat de Garilhe,M., Bell. Soc.Chem.Biol. 51, 1511 (1969).

15. Cushley,R.J., Wanatabe,K.A., and Fox,J.J., J.Am. Chem.Soc. 89, 394 (1967).

16. Bergman,W., and Feeney,R.J., ibid, 72, 2809 (1950).

17. Cohen,S.S., Prog.Nuc.Acid.Res. and Mol.Biol. 5, 1 (1966).

18. Codington,J.F., Cushley,R.J., and Fox,J.J., J.Org.Chem. 23, 466 (1968).

19. Belyanchikova,N.I., Doklady Biological Sciences, Jan.-Feb. 1969, p.54.

20. Lett,J.T., Caldwell,I., and Little,J.G., J.Mol.Biol. 48, 395 (1970).

21. Morris, Cramer, Exp.Cell.Res. 51, 555 (1968).

22. Dethlefs,L.A., Cancer Res. 29A, 1717 (1969).

23. Ogilvie,K.K., and Iwacha,D., Can.J.Chem. 48, 862 (1970).

24. Nagyvary,J., and Provenzale,R.G., Biochemistry 8, 4769 (1969).

25. Fox,J.J., Miller,N., and Wempen,I., J.Med.Chem. 9, 101 (1966).

26. Imazawa,M., and Ueda,T., Tetrahedron Letters 55, 4807 (1970).

27. Falco,E.A., Otter,B.A., and Fox,J.J., J.Org.Chem. 35, 2326 (1970).

28. Lehninger,A.L., Biochemistry, Worth Publishers, N.Y., 1970, p.242.

29. Jardetzky,C.D., and Jardetzky,O., J.Amer.Chem.Soc. 82, 222 (1960).

30. Chargaff,E., and Davidson,J.N., "Nucleic Acids" I, Acad.Press, N.Y., 1955.

31. Miles,H.T., Biochem.Biophys.Act. 27, 46 (1958).

32. Pullman,B., and Pullman,A., Bull,soc.chim.France 973 (1958).

33. Pullman,A., and Pullman,B., Compt.Rend. 246, 611 (1957).

34. Kardetzky,O., Biopolymers 1, 501 (1964).

35. Kokko,J.P., Mandell,L., and Goldstein,J.H., J.Am. Chem.Soc. 84, 1042 (1962).

36. Becker,E.D., Miles,H.T., and Bradley,R.B., J.Am. Chem.Soc. 87, 5575 (1965).

37. Katritzky,A.R., and Waring,A.J., J.Chem.Soc. 3046 (1963).

38. Reddy,G.S., Hobgood,R.T., and Goldstein,J.H., J.Am.Chem.Soc. 84, 336 (1962).

39. Jones,A.J., Winkley,M.W., Grant,D.M., and Robins,R.K., Proc.Nat.Acad.Sci. 65, 27 (1970).

40. Jones,A.J., Grant,D.M., Winkley,M.W., and Robins,R.K., J.Phys.Chem. 74, 2684 (1970).

41. Jones,A.J., Grant,D.M., Winkley,M.W., and Robins,R.K., J.Amer.Chem.Soc. 92, 4079 (1970).

42. Jones,A.J., Winkley,M.W., and Grant,D.M., Tetrahedron Letters 59, 5197 (1969).

43. Musher,J.I., J.Chem.Phys. 43, 4081 (1965).

44. Jackman,L.M., and Sternhell,S., Applications of Nuclear Magnetic Resonance Spectroscopy in Organic Chemistry, Pergammon Press, N.Y., 1969, Part 2, p.104.

45. Jackman,L.M., and Sternhell,S., ibid, p.114.

46. Bovey,F.A., Nuclear Magnetic Resonance Spectroscopy, Academic Press, N.Y. (1969) p.88.

47. Sternhell,S., Quarterly Reviews 23, 236 (1969).

48. Karplus,M., J.Chem.Phys. (1959) 30, 11.

49. Karplus,M., ibid, 85, (1963) 2870.

50. Cohen,A.D. and Schaefer,T., Mol.Phys. (1966) 10, 209.

51. Bothner-By,A.A., in 'Advances in Mag.Res.', ed. Waugh,J.S., Academic Press, N.Y. 1965, vol.1.

52. Abraham,R.J., in 'Nuclear Magnetic Resonance for Organic Chemists', ed. Mathieson,D.W., Acad.Press, N.Y., 1967.

53. Jackman,L.M., and Sternhell,S., 'Applications of n.m.r. spectroscopy in organic chemistry', Pergammon Press, Oxford, 1968, Part 4, p.283.

54. Lazlo,P., and Musher,J.I., Bull.Soc.Chim.France, 2558 (1964).

55. Barfield,M., J.Amer.Chem.Soc. 93, 1066 (1971).

56. Sternhell,S., Rev.Pure Appli.Chem. 14, 15 (1964).

57. Inoue,Y., and Kakanishi,K., Biochem.Biophys.Acta 120, 311 (1966).

58. Glascoe,P.K., and Long,F.A., J.Phys.Chem. 64, 188 (1960).

59. Blackburn,B.J., Grey,A.A., Smith,I.C.P., and Hruska, F.E., Can.J.Chem. 48, 2866 (1970).

60. Anderson,W.A., and Freeman,R., J.Chem.Phys., 37, 85 (1962).

61. Freeman,R., Anderson,W.A., J.Chem.Phys. 37, 2053 (1962).

62. Ts'o,P.O.P., Schweizer,M.P., and Hollis,D.P., Ann. New York Acad.Sci. 158, 266.

63. Gatlin,L., and Davis,J.C., J.Amer.Chem.Soc. 84, 4464 (1962).

64. Lemieux,R.U., Can.J.Chem. 39, 116 (1960).

65. Lemieux,R.U., and Hoffer,M., ibid 39, 110 (1961).

66. Lemieux,R.U., and Lineback,D.R., Ann.Rev.Biochem. 32, 155 (1963).

67. Hall,L.D., Steiner,P.R. and Pedersen,C., Can.J.Chem. 48, 1155 (1970).

68. Abraham,R.J., and McLauchlan,K.A., Mol.Phys. 5, 513 (1962).

69. Jardetzky,C.D., J.Amer.Chem.Soc. 82, 229 (1960).

70. Jardetzky,C.D., ibid., 84, 62 (1961).

71. Steiner,P.R., M.Sc.Thesis, UBC, 1969.

72. Abraham,R.J., Hall,L.D., Hough,L., and McLauchlan,K.A., J.Chem.Soc. 3699 (1962).

73. Hendrickson,J.B., Org.Biol.Chem. 83, 4537 (1961).

74. Goldstein, Tetrahedron 1969, p.877.

75. Wasylishen, R., private communication.

76. Prestegard,J.H., and Chan,S.I., J.Amer.Chem.Soc. 90, 1042 (1968).

77. Donahue,J., and Trueblood,K.N., J.Mol.Biol. 2, 263 (1960).

78. Hruska,F.E., J.Amer.Chem.Soc. 93, 1795 (1971).

79. Dugas,H., Blackburn,B.J., Robins,R.K., Deslauriers,R., and Smith,I.C.P., J.Amer.Chem.Soc. 93, 3468 (1971).

80. Emsley,J.W., Feeney,J., and Sutcliffe,L.H., High Resolution NMR Spectroscopy Vol.2, Pergammon Press, New York, 1966.

81. ApSimon,J.W., Craig,W.G., Demarco,P.V., Mathieson,D.W., Nasser,A.K.G., Saunders,L., and Whalley,W.B., Chem.Comm., 1966, 754.

82. ApSimon,J.W., Craig,W.G., Demarco,P.V., Mathieson,D.W., Saunders,L., and Whalley,W.B., Tetrahedron, 23, 2339 (1967).

83. ApSimon,J.W., Craig,W.G., Demarco,P.V., Mathieson,D.W., Saunders,L., and Whalley,W.B., Tetrahedron 23, 2357 (1967).

84. ApSimon,J.W., Craig,W.G., Demarco,P.V., Mathieson,D.W., and Whalley,W.B., Tetrahedron 23, 2375 (1967).

85. ApSimon,J.W., Demarco,P.V., Mathieson,D.W., Craig,W.G., Karim,A., Saunders,L., and Whalley,W.B., Tetrahedron 26, 119 (1970).

86. Lemieux,R.U., and Stevens,J.D., Can.J.Chem. 43, 2059 (1965).

87. Hall,L.D., and Manville,J.F., and Bhacca,N.S., Can.J.Chem. 47, 1 (1969).

88. Sundaralingam,M., Biopolymers. 7, 821 (1969).

89. Lakshminarayanan,A.V., and Sasisekharan,V., Biochim. Biophys.Acta 204, 49 (1970).

90. Tsuboi,M., Kuriyagawa,F., Matsuo,K., Kyogoku,Y., Bull.Chem.Soc.Jap. 40, 1813 (1967).

91. Rogers,G.T., and Ulbricht,T.L.V., Biochem.Biophys. Res.Comm. 39, 414 (1970).

92. Rogers,G.T., and Ulbricht,T.L.V., ibid, 39, 419 (1970).

93. Miles,D.W., Hahn,S.J., Robins,R.K., Robins,M.J., and Eyring,H., J.Phys.Chem. 72, 1483 (1968).

94. Saenger,W., and Scheit,K.H., J.Mol.Biol. 50, 153 (1970).

95. Schweizer,M.P., Witowski,J.T., and Robins,R.K., J.Amer.Chem.Soc. 93,277 (1971).

96. Castellano,S., and Bothner-By,A.A., J.Chem.Phys. 41,3863 (1964).

97. Bothner-By,A.A., and Castellano,S., LAOCN3, Mellon Institute, Pittsburgh, Pa., 1966.

98. Hruska,F.E., Can.J.Chem., 49,2112 (1971).

99. Miles,D.W., Inskeep,W.H., Robins,M.J., Winkley,M.W., Robins,R.K., and Eyring,H., J.Amer.Chem.Soc. 92,3872 (1970).

100. Barfield,M., and Chakrabarti,B., Chem.Rev. 69, 757 (1969).

101. Brown,D.M., Cochran,W., Medlin,E.H., and Varadarajan,S., J.Chem.Soc. 868 (1967).

102. Doerr,I.L., Cushley,R.J., and Fox.J.J., J.Org.Chem., 33,1592 (1968).

103. Tougard,P., Biochem.Biophys.Acta 37,961 (1969).

104. Lynden-Bell,R.M., and Harris,R.K., Nuclear Magnetic Resonance Spectroscopy, Nelson, London 1969

105. Culvenor,C.C.J., Heffernan,M.L., and Woods,W.G., Aust.J.Chem. 18, 1605 (1965).

106. Pachler,K.G.R., Tollenaere,J.P., and Wessels,P.L., Tetrahedron 25, 5255 (1969).